USING THE ECG TO PREDICT CARDIAC REARREST

by

LAKEN S. IRISH

Submitted in partial fulfillment of the requirements for the degree

Master of Science

Department of Biomedical Engineering

CASE WESTERN RESERVE UNIVERSITY

August 2023

Committee Members

CASE WESTERN RESERVE UNIVERSITY SCHOOL OF GRADUATE STUDIES

We hereby approve the thesis of:

Laken S. Irish

candidate for the degree of **Master of Science***.

Committee Chair:

Dominique Durand, PhD

Committee Members:

Lance Wilson, MD, Kenneth Laurita, PhD, Kenneth Loparo, PhD

Date of Defense:

July 10, 2023

*We also certify that written approval has been obtained for any proprietary material contained therein.

Dedication

I dedicate this thesis to all those who have perished from sudden cardiac arrest, particularly those represented in this study. I hope your contributions ultimately help to improve the lives of others. And to the families of loved ones lost to sudden cardiac arrest, may you find peace and comfort in your memories and time.

God bless.

~~~~~~

Finally, I dedicate this thesis to my dearly loved and departed friend Brian, who passed away from an overdose in May 2022.

May God bless you, Brian – you are so painfully missed!

"Wildflower seed on the sand and wind,

May the four winds blow you home again!"

- Robert Hunter, Jerry Garcia

~~~~~~

Table of Contents

Cardiac Arrest and Rearrest: *18*

ECG Biomarkers of Cardiac Arrest & Rearrest: *21*

Depolarization Parameters to Predict Cardiac Outcomes: *21*

Repolarization Parameters to Predict Cardiac Outcomes: *23*

Prediction with Machine Learning: *27*

Hypothesis: *29*

Figure 1: *30*

Figure 2: *30*

Figure 3: *31*

Figure 4: *31*

Overview: *32*

Figure 5: *33*

Data Collection: *33*

ECG Processing: *34*

Figure 6: *35*

Figure 7:…… 36

Figure 8:…… 37

Figure 9:…… 38

Figure 10:…… 38

Calculation of RR Variability Features for ML:…… 37

Figure 11:…… 42

Figure 12:…… 43

Calculation of Repolarization Variability Features for ML:…… 43

Figure 13:…… 45

Figure 14:…… 46

Figure 15:…… 49

Table 1:…… 51

Figure 16:…… 50

Table 2:…… 52

Table 3:…… 53

Table 4:…… 54

Input Data and Cross Validation Settings: 54

Classifier Selection Options: 56

Table 5: 58

Machine Learning Models: 58

Performance Metrics Chosen: 59

Patient Population Characteristics: 60

Survival by Primary and Rearrest Rhythms: 61

Table 6: 61

Figure 17: 63

Figure 18: 63

Machine Learning to Predict Rearrest Occurrence with RR Variability Features: 64

Table 7: 65

Figure 19: 66

Effect of Adding Repolarization Variability Features to RR Variability to Predict Rearrest Occurrence: 66

Figure 20: 69

Figure 21:..... 69

Effect of Adding Repolarization Features to Predict Rearrest Type:..... 70

Figure 22:..... 70

Table 8:..... 72

Figure 23:..... 73

RR Variability to Predict Rearrest Occurrence – Comparison to Prior Studies:..... 75

Figure 24:..... 74

Addition of Repolarization Variability Features to Predict Rearrest Occurrence & Type:..... 78

Non-Linear Repolarization Features & Entropy:..... 80

Clinical Implications from Machine Learning:..... 82

Conclusions:..... 84

Future Directions:..... 85

List of Tables

Table 1: List of features measured on RR interval and repolarization series..... 51

Table 2: Equations for time domain features measured on RR interval and repolarization series..... 52

Table 3: Equations for frequency domain features measured on the RR interval series..... 53

Table 4: Equations for non-linear features measured on RR interval and repolarization series..... 54

Table 5: Summary of the five machine learning problems we addressed in this study. We varied the model type, feature set, the use of feature selection and the response type to address the research question..... 58

Table 6: ECG characteristics, demographics, and arrest characteristics by rearrest type. The groups are well matched, and no significant differences exist..... 61

Table 7: Classifier performance compared to Elola et al, who also used RR variability features calculated from the ECG to predict cardiac rearrest occurrence..... 65

Table 8: Performance metrics for a 10-fold CV, multiclass, linear SVM using RR variability features, all features (RR and repolarization), and the top 25 ANOVA ranked features, respectively, to predict rearrest type. Green boxes indicate

performance improvements, while red indicates worsening performance when compared to the classifier using RR variability features only. 72

List of Figures

Figure 1: The four different mechanisms causing cardiac arrest and rearrest. 30

Figure 2: Action potentials and calcium transients recorded from a rabbit ventricular myocyte. Panel A shows pacing induced action potential duration alternans (top) and alternating calcium transients (bottom). Panel B shows the same, except the cell is voltage clamped. No action potential duration alternans are present, however alternating calcium transients still exist, suggesting that abnormalities in calcium handling – not membrane voltage – cause APD alternans. Adapted from Chudin E., Goldhaber J., Garfinkel A., Weiss J., Kogan B. Biophysical Journal 1999; 77: 2930-2941 30

Figure 3: Relating ECG T-wave alternans (left) and action potential duration (APD) alternans. T-wave alternans (TWA) typically present as microvolt changes in amplitude. APD alternans that underlie TWA are much larger. Adapted from Cutler MJ, Rosenbaum DS. Heart Rhythm 2009; 6: S22-S28 31

Figure 4: Mechanisms of concordant and discordant cellular action potential alternans. Concordant alternans (left) present as an in phase long-short-long pattern from location A to B on the myocardium. The spatial repolarization gradient given by the vertical dotted lines is relatively small. A premature beat (*)

travels slowly through repolarized tissue to location B. This prolongs the diastolic interval, increasing the APD at location B, and leading to spatially out of phase, or discordant, alternans. Spatial dispersion of repolarization is greatly increased (red, shaded area), leading to slow conduction. With another premature beat, conduction is blocked due to refractoriness at B, and the impulse propagates around it, creating a reentrant circuit, and causing ventricular fibrillation. Adapted from Wilson LD, Rosenbaum DS. Europace 2007; 9: vi77-vi82. ..... *31*

Figure 5: An overview of the methods for using RR variability and repolarization features derived from the ECG to predict cardiac rearrest occurrence and mechanism. *33*

Figure 6: Annotations (purple lines) identifying the indices of the mid-PQ isoelectric (I) point, R-wave (R) and T-wave (T) peaks on a sample beat from a representative ECG. *35*

Figure 7: Original ECG with high frequency noise (left) and after low-pass filtering (right). *36*

Figure 8: Original ECG (left, blue) with baseline wander estimated by a cubic spline (black) fit to mid-PQ isoelectric points and after removal by subtracting the spline (right). *37*

Figure 9: The RR interval series (red bidirectional arrow) on a representative ECG. 38

Figure 10: RR Interval series taken from the period of ROSC for a patient who had a VT/VF rearrest..... 38

Figure 11: Panel A – Normalized ECG from a patient with bigeminy who had a PEA rearrest. Panel B – Resampled RR interval series. The short-long-short pattern from bigeminy is apparent. Panel C – The resulting Welch periodogram over the traditional physiologic range. The blue shaded region indicates the low frequency band, while red indicates the high frequency band..... 42

Figure 12: A Poincaré plot for a patient who did not rearrest (yellow stars) and a patient who had a PEA rearrest (pink squares). Feature SD1 measures variability along the red dotted line while feature SD2 measures variability along the blue dotted line..... 43

Figure 13: Beat level measurements that constitute the T-wave amplitude, QT interval and repolarization area series'..... 45

Figure 14: T-wave amplitude series from a representative 2-minute ECG trace. 46

Figure 15: Panel A – Simulated ECG with TWA present in the first half and no amplitude oscillations present in the second half. Panel B – The T-wave amplitude

series. Panel C – The time varying amplitude series, a(t), after complex demodulation of the T-wave..... 49

Figure 16: T-wave amplitude oscillations at frequencies of every other beat or 1/2 (top), every third beat or 1/3 (middle), and every fourth beat or 1/4 (bottom). Oscillation amplitude is represented by the red bidirectional arrows..... 50

Figure 17: Panel A –Percent survival by primary arrest type. Panel B – Percent survival by rearrest type. Patients who have a VT/VF primary or rearrest type have the greatest odds of survival..... 63

Figure 18: Panel A – Arrest Etiology by rearrest group. Etiology is analyzed as two separate groups: cardiac or respiratory, which also includes overdose, drowning, and others. Etiology was predominantly cardiac for patients who had a VT/VF rearrest. Panel B – Primary arrest type by rearrest type. Most patients who had a VT/VF rearrest had VT/VF primary arrest..... 63

Figure 19: Receiver operating curves and model operating points for a linear SVM classifier (left) and an adaptive boosted (AdaBoost) decision tree classifier (right). Both classifiers predict cardiac rearrest occurrence using only RR variability features. The AdaBoosted decision tree model had improved performance over the linear SVM model..... 66

Figure 20: Receiver operating curves for the linear SVM models used to predict rearrest occurrence without feature selection (left) and with feature selection (right), using the top 25 ANOVA ranked features. 69

Figure 21: Representative confusion matrices for the linear SVM classifiers with RR variability features only (left) and the top 25 ANOVA ranked features (right) to predict rearrest occurrence. The true positive rate for the rearrest class improved by over10% when repolarization features were added, and feature selection was used. Hues of blue indicate true positive rates, with dark blue representing the highest true positive rate. Hues of orange represent false positive/negative rates, with dark orange representing the highest false positive/negative rate..... 69

Figure 22: The top 25 features identified by the ANOVA ranking algorithm used in the Linear SVM classifier to predict cardiac rearrest occurrence. Features were selected from the combined RR variability and repolarization feature set. Repolarization features comprise 44% of the top 25. Measures of entropy comprise nearly a quarter of the top 25. The distribution of time, frequency and non-linear features is 36%, 16%, and 48%, respectively. 70

Figure 23: Representative confusion matrices for the 10-fold CV, multiclass, linear SVM classifiers using RR variability features only (left), and the top 25 ANOVA

ranked features (right) to predict rearrest type. Hues of blue indicate true positive rates, with dark blue representing the highest true positive rate. Hues of orange represent false positives/negative rates, with dark orange representing the highest false positive/negative rate. The propensity of the model to classify observations as no rearrest (No RA) increases when using the top 25 ANOVA ranked features..... 73

Figure 24: The top 25 most important features identified by the ANOVA ranking algorithm used in the 10-fold CV, multiclass, linear SVM. Features were selected from the combined RR variability and repolarization feature set. Repolarization features comprise 40% of the top 25. Measures of entropy comprise 20% of the top 25, and 40% of the top repolarization features. The distribution of time, frequency and non-linear features is 24%, 24%, and 52%, respectively..... 74

Acknowledgements

Thank you to my colleagues at MetroHealth MC: Gary Pawlowski, Brendan Morgan, Adrienne Dennis, Lydia Akino, and Julie Nichols. I appreciate your help, support, and friendship. Thank you to Drs. Ohad Ziv, Soufian AlMahameed, and Joe Piktel for your time, feedback, and interest in my work. Also to Dr. Dominique Durand and Dr. Kenneth Loparo for your mentorship on this thesis project.

Dr. Robert Morgan: thank you for your friendship, support, and guidance!

Dr. Ed Lesnefsky: thank you for supporting me and sending alternans articles in the mail - ripped straight from the journal!

A special thank you to my wonderful boyfriend Joey Lesnefsky. You more than anyone inspire me to be the best scientist – and person – I am capable of being. I'm so grateful for your love and support.

Finally, **a very big thank you** to my great mentors Dr. Kenneth Laurita and Dr. Lance Wilson. You've both dedicated a lot of time and effort to developing my skills and helping me navigate my path forward and I appreciate that more than I can say.

Using the ECG to Predict Cardiac Rearrest

Abstract

By

LAKEN S. IRISH

Recurrent cardiac arrest, or cardiac rearrest, remains a significant barrier to successful resuscitation from cardiac arrest and is associated with worse outcomes. Metrics calculated from the electrocardiogram, including heart rate variability (RR variability) and repolarization variability, have been associated with cardiac arrest occurrence and arrhythmias. These metrics, called features, were utilized in a machine learning model to test the hypothesis that combining repolarization variability features with RR variability features can improve the prediction of cardiac rearrest occurrence and its type: no rearrest, pulseless electrical activity rearrest, and pulseless ventricular tachycardia/fibrillation rearrest. Repolarization features enhanced prediction of rearrest occurrence as evidenced by increased specificity and validation accuracy but failed to improve prediction of rearrest type. Analysis of variance revealed that repolarization features were associated with rearrest occurrence and type. With further development and refined clinical implementation,

machine learning models represent a potential novel method of predicting rearrest and improving resuscitation outcomes.

Introduction

Cardiac Arrest and Rearrest:

Cardiac arrest (CA) is a medical emergency that occurs when the heart suddenly and unexpectedly stops beating, resulting in circulatory failure, end organ ischemia, particularly to the heart and brain, and death[1]. As many as 300-450,000 Americans every year suffer CA[1,2]. Tragically, it is often the first manifestation of underlying cardiovascular disease, resulting in death typically within minutes if left untreated[1]. Successful resuscitation from CA requires rapid intervention by emergency medical services (EMS) with initiation of advanced cardiac life support (ACLS) therapies including cardiopulmonary resuscitation (CPR), administration of vasopressors (epinephrine), antiarrhythmics, and defibrillation or cardioversion of malignant ventricular arrhythmias[3,4].

There are 4 different mechanisms (types) of CA: ventricular fibrillation (VF), pulseless ventricular tachycardia (VT), pulseless electrical activity (PEA) and asystole[4]. In VF, there is no organized electrical ventricular activity, resulting in no effective myocardial contraction and no pulse[5]. On the electrocardiogram (ECG), VF looks

chaotic with deflections that vary in shape and amplitude[5]. Sustained VT is characterized by ventricular beats typically occurring at a rate of 150-300 beats per minute, causing a significant decrease in cardiac output leading to pulseless VT and CA. PEA is also known as electromechanical dissociation, where electrical activity is relatively normal, but there is a disturbance in contraction[4,6]. Asystole is a total absence of atrial and ventricular electrical and contractile activity: the classic "flatline" ECG[5]. Figure 1 shows representative ECG traces of the four arrhythmias causing CA.

If a patient is resuscitated from CA, a return of spontaneous circulation (ROSC) is achieved. However, CA can occur again soon after ROSC (rearrest), typically within the time period up to hospital admission[7]. The problem of rearrest affects 30-80% of successfully resuscitated patients and is associated with low rates of survival to hospital discharge[7,8]. As rearrest is associated with poor outcomes, preventing, or effectively treating it is an opportunity to intervene and improve CA outcomes.

It is important to note that ACLS treatment guidelines differ depending on the type of CA[3]. Since VT and VF are abnormal ventricular rhythms (arrhythmias) that result from disturbances in impulse formation and impulse conduction[5,9], their treatments are similar. For VT/VF, ACLS guidelines indicate prompt CPR, defibrillation

(VF) or cardioversion (VT), and administration of vasopressors and antiarrhythmics[3,5,9]. Because of the similarity in causes and management of PEA and asystole, they are grouped together under ACLS treatment guidelines[3,4]. These treatments include CPR and vasopressors[3,4]. Specific treatments are oftentimes not initiated until after the onset of rearrest, once the type (e.g., VF, PEA, etc.) is known. If impending rearrest and its mechanism were apparent prior to onset, targeted treatments could be initiated, leading to abatement or prevention of rearrest altogether. This would improve survival rates and diminish the extent of myocardial and brain injury caused by rearrest. Moreover, knowledge of the rearrest type would be necessary for successful abatement/prevention of rearrest, because treatments for PEA and VT or VF are diametrically opposed. For example, treatments for PEA including vasopressors, epinephrine, and catecholamines can cause VT/VF, whereas treatments for VT/VF such as antiarrhythmics (amiodarone) and beta blockers may worsen or cause PEA[9,10]. Herein lies the gap in knowledge: it is unknown if rearrest and its type can be predicted such that early treatment therapies could be implemented to improve resuscitation outcomes.

ECG Biomarkers of Cardiac Arrest & Rearrest:

The ECG is the heart's electrical activity as it appears on the body surface and is routinely measured to monitor the health of a patient's heart[3]. More specifically, the ECG depicts changes in body surface voltage waveforms that are generated by depolarization and repolarization of the heart's cells[5]. An ECG recording is *always* performed on CA patients to provide an ongoing, real-time, and sensitive measure of heart rhythm. Numerous cardiac pathologies can be made with an ECG including metabolic and electrolyte disturbances, myocardial ischemia, structural remodeling, and arrhythmias including those that cause CA/rearrest[5]. Additionally, the ECG has been used to stratify long term risk of sudden CA.

Depolarization Parameters to Predict Cardiac Outcomes:

Coordinated depolarization through the ventricle of the myocardium, as evidenced by a narrow QRS wave, is necessary for effective cardiac output. Abnormalities of myocardial depolarization have been associated with poor cardiac outcomes[11,12,13]. Late potentials are given by low amplitude deflections at the end of the QRS complex on the ECG[11]. These deflections represent delayed conduction through diseased myocardium potentially due to genetic causes, ischemia, or other

cardiomyopathies, and provide a substrate for reentrant ventricular arrhythmias[11]. Although the presence of late potentials has shown increased risk for VT/VF, the amplitude of ECG deflections is small, making them difficult to identify[11]. For this reason, an improved approach to identifying depolarization abnormalities that are linked to CA/rearrest is needed. The ECG R-wave represents depolarization of the myocardium, and the RR interval, or cycle length is analogous to instantaneous heart rate. Heart rate variability (HRV) is the fluctuation of the time intervals between heartbeats and is a measure of neurocardiac regulation, generated by heart-brain interactions through the autonomic nervous system[14]. Heart rate varies to provide rapid compensation in cardiac output needed to respond to demands in the external or internal environment, such as stress or exercise, in order to maintain homeostasis. Disease states can negatively impact this flexibility, by increasing or decreasing HRV beyond normal physiological limits[14]. Note that traditional HRV measurements are analyzed on ECGs in sinus rhythm without ectopic beats, allowing for the measure to reflect autonomic regulation of heart rate more specifically. Studies have shown that abnormal HRV has been associated with multiple pathologies including myocardial infarction and myocardial dysfunction, which can increase the risk of CA[1,13]. *Huikuri et al* identified multiple studies that found associations between HRV and sudden CA[12].

Other studies have more specifically identified acutely decreased HRV preceded both sustained and non-sustained VT and VF[15,16,17]. Importantly, in the peri-cardiac arrest setting, a variant of HRV (measuring RR variability on available beats, regardless of underlying rhythm) has successfully been used in machine learning models to predict in-hospital-CA due to PEA[18] and the occurrence of rearrest after out-of-hospital-CA[19]. These studies suggest the possibility of using RR interval metrics as a biomarker for predicting rearrest occurrence and rhythm type.

Repolarization Parameters to Predict Cardiac Outcomes:

Other ECG waveforms such as the T-wave, which represent myocardial repolarization, show predictive promise as well. Abnormalities in repolarization measures on the ECG have been established in patients with conditions that can cause CA. Prolongation of the QT interval may result from genetic disorders like the Long QT syndromes, drug toxicity, metabolic imbalances such as hypokalemia, or certain types of heart block, and can cause VT or VF to develop[1,5,9,20]. Abnormalities in the ST segment and T-wave including diminished or elevated amplitude and inverted morphology are also observed in conditions like acute coronary syndromes, which are

a common cause of CA/rearrest[1,5,9,21-22]. These data indicate the potential utility of the QT interval and T-wave amplitude as positive predictors for rearrest.

Importantly, variability or dynamic oscillations of the T-wave have also been associated with cardiac pathology. For example, repolarization or T-wave alternans (TWA), defined as a beat-to-beat fluctuation in the amplitude or morphology of the ST segment and/or T-wave, has also been associated with risk of arrhythmia development. Studies have shown TWA to precede VT or VF in patients with varying pathologies including long QT syndrome, myocardial infarction, heart failure, pericardial effusion, and electrolyte derangements[21,23,24]. That TWA can predict arrhythmias consistently across numerous clinical diseases and experimental models, supports its potential as a positive predictor for arrhythmias causing CA/rearrest[23-27]. ECG TWA is mostly a manifestation of alternating calcium transient amplitude caused by dysfunctional proteins involved in calcium-induced-calcium-release (CICR)[9,26,28-34]. Mechanistically, alternations in the calcium transient lead to action potential (AP) shortening/prolongation (AP duration, or APD, alternans) via calcium-dependent repolarization currents active during phases 2 and 3 of the action potential (AP). This links cellular calcium alternans to the process of repolarization, which ultimately manifests as alternans of the T-wave on an ECG[9,23,24,28-30,32,33,35,36]. Figure 2, adapted

from *Chudin et al*, illustrates how APD alternans is caused by calcium transient alternans.

When APD alternans initially develops, APs of a particular duration (shortened or prolongated) are concordant, or in phase across all cells of a particular region. This manifests as alternating T-wave amplitude (2:1 alternans) on the surface ECG (Figure 3). During concordant alternans, an ectopic beat or increase in heart rate can trigger APs in a particular region to become discordant, or spatially out of phase with those in a neighboring region (Figure 4). Discordant alternans greatly increases spatial dispersion of repolarization which increases the tissue's susceptibility to conduction block, reentrant excitation and thus arrhythmias like VT and VF[25,26,28,29,35,38]. On the surface ECG, discordant APD alternans manifest as T-wave amplitude oscillating at lower frequencies (3:1, 4:1) or in a more complex pattern[24,25]. Complex T-wave amplitude oscillations may therefore be a biomarker for impending VT/VF rearrest. This hypothesis is further supported by preliminary data from an *in vivo* translational resuscitation model where 90% of all VT/VF rearrest events were preceded by complex T-wave oscillations.

Examining the clinical conditions associated with PEA may suggest evidence for an ECG biomarker that can be used to predict it. Studies have found that up to 50% of primary PEA rhythms were attributable to a cardiac event, suggesting ischemia may be important to developing PEA[39]. It has also been shown that PEA can occur following prolonged VF that was successfully terminated by defibrillation. In this case, prolonged VF provides a substrate for metabolic and electrolyte disturbances that could support the development of PEA[39]. Derangements in calcium handling have been implicated in PEA, since intracellular calcium is critical for myocardial contraction, which is severely impaired during PEA[6,39]. Ischemia and metabolic derangements impair cellular calcium handling and are known to trigger concordant TWA. TWA has also been associated with experimental and human heart failure, in which the central feature is impaired myocardial calcium handling. Given that impaired calcium handling underlies concordant TWA and PEA, we contend that concordant TWA may be a positive marker for PEA in the CA/rearrest setting. Preliminary data in an *in vivo* translational resuscitation model further supports this hypothesis, where 88% of all PEA rearrest events were preceded by concordant TWA. To date, there is no reliable method to predict rearrest occurrence and rhythm type.

Prediction with Machine Learning:

Machine learning (ML) is a branch of artificial intelligence that aims to find generalizable, predictive patterns in data. Classification is a type of ML that predicts categorical outcomes or classes by using input metrics known as features that are calculated on a population of interest. Individuals belonging to a population are assigned a class label that describes the group or class they belong to, and features that characterize the individual are calculated or recorded. Features can be quantitative or qualitative descriptors of the individual being studied. The ML model works by identifying patterns in the features that characterize individuals belonging to the same class. The ML model then derives a mathematical function that serves as a boundary to distinguish and separate the classes. ML models use multiple subsets of the population data, known as training data, to find the best possible boundary that separates the classes. The performance of the model can be assessed by how well it correctly classifies a different subset of the population data, known as testing data. A process known as cross-validation (CV) determines how the population data is divided for training and testing. Sometimes calculated features are unrelated to the output classes, or otherwise do very little to distinguish them. ML models can be overfitted if redundant or unrelated features are used. Models that are overfit tend to be less

generalizable, leading to poor performance and higher misclassification. In cases like this, feature selection can be used to identify features that are strongly correlated or associated with the output classes. Getting rid of features that are unrelated to the output class or otherwise redundant improves the performance of the model. In addition to improving the predictive capacity of the ML model, the features identified as strongly correlated with the output can provide insight into important phenomena that underlie the population data and serve to differentiate the classes.

Multiple studies have used features calculated from cardiac action potentials[40] or the ECG[18,41] in ML models to predict CA occurrence or CA outcomes including survival. The models in these studies showed strong predictive capacity, with performance metrics such as the area under the receiver operating curve (AUROC) values exceeding 85%. Importantly, only one study to date has used a ML model to successfully predict occurrence of rearrest on successfully resuscitated out-of-hospital CA patients using features measured on the ECG[19]. *Elola et al* reported a median AUROC of 69% for predicting rearrest occurrence[19]. Together, these studies suggest that ML models have the potential to predict rearrest and its mechanism (VT/VF, PEA, etc.) from features measured on a surface ECG.

Hypothesis:

We hypothesize that, with a machine learning model, ECG repolarization variability features will enhance the predictive capability for cardiac rearrest occurrence *and* cardiac rearrest type (PEA rearrest, or VT/VF rearrest), compared to RR variability features alone.

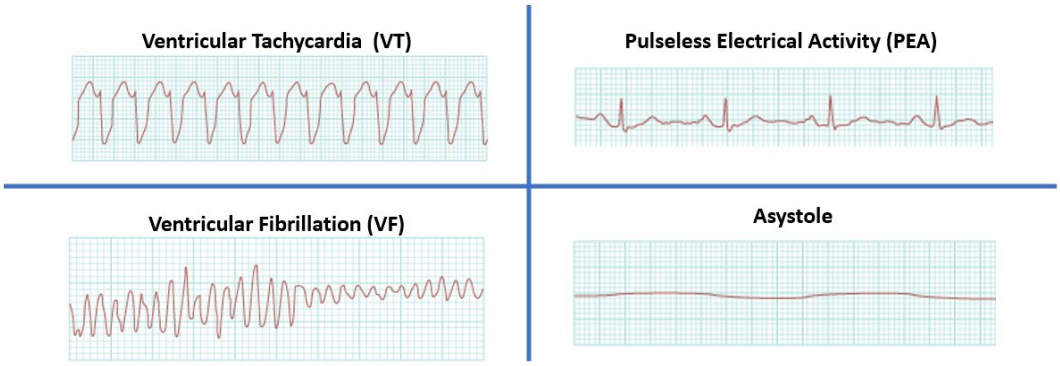

Figure 1: The four different mechanisms causing cardiac arrest and rearrest.

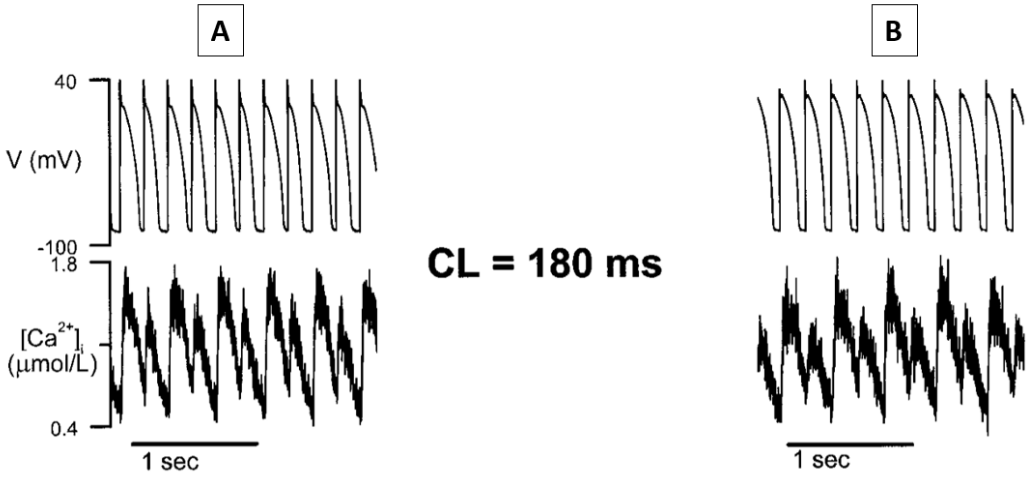

Figure 2: Action potentials and calcium transients recorded from a rabbit ventricular myocyte. Panel A shows pacing induced action potential duration alternans (top) and alternating calcium transients (bottom). Panel B shows the same, except the cell is voltage clamped. No action potential duration alternans are present, however alternating calcium transients still exist, suggesting that abnormalities in calcium handling – not membrane voltage – cause APD alternans. Adapted from Chudin E., Goldhaber J., Garfinkel A., Weiss J., Kogan B. Biophysical Journal 1999; 77: 2930-2941

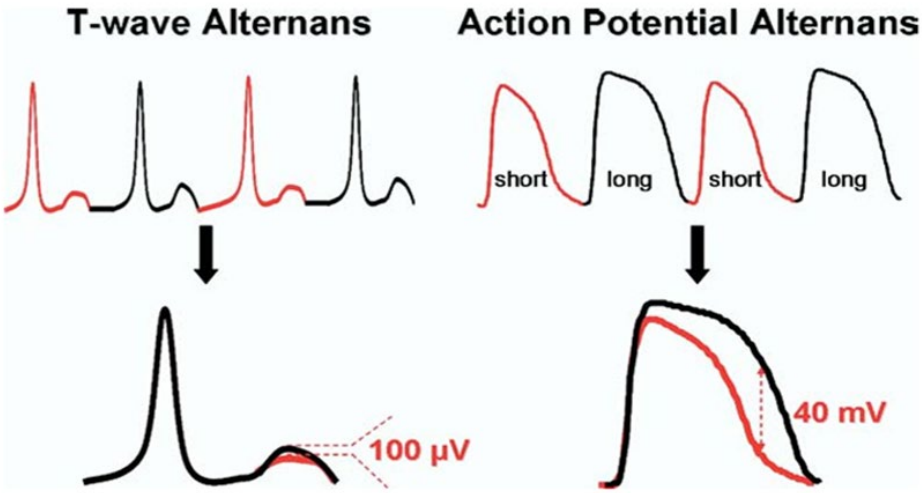

Figure 3: Relating ECG T-wave alternans (left) and action potential duration (APD) alternans. T-wave alternans (TWA) typically present as microvolt changes in amplitude. APD alternans that underlie TWA are much larger. Adapted from Cutler MJ, Rosenbaum DS. Heart Rhythm 2009; 6: S22-S28

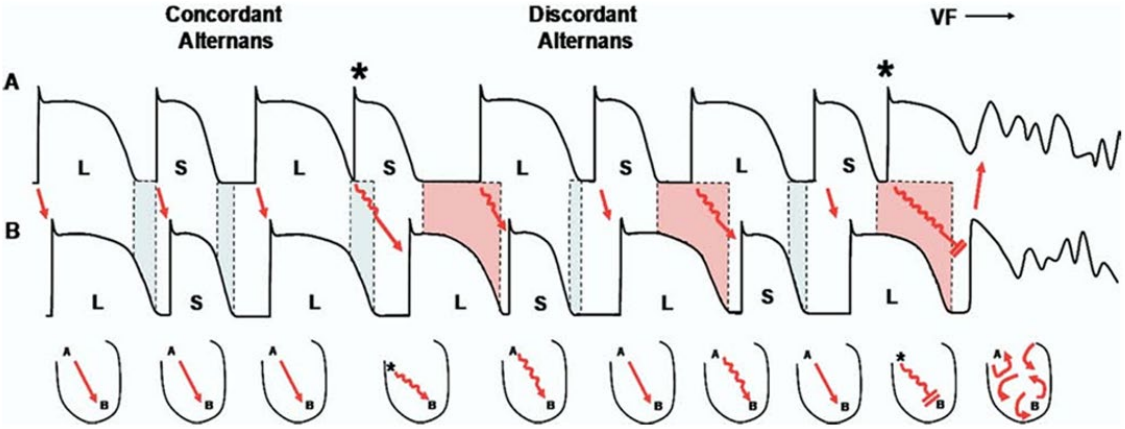

Figure 4: Mechanisms of concordant and discordant cellular action potential alternans. Concordant alternans (left) present as an in phase long-short-long pattern from location A to B on the myocardium. The spatial repolarization gradient given by the vertical dotted lines is relatively small. A premature beat (*) travels slowly through repolarized tissue to location B. This prolongs the diastolic interval, increasing the APD at location B, and leading to spatially out of phase, or discordant, alternans. Spatial dispersion of repolarization is greatly increased (red, shaded area), leading to slow conduction. With another premature beat, conduction is blocked due to refractoriness at B, and the impulse propagates around it, creating a reentrant circuit, and causing ventricular fibrillation. Adapted from Wilson LD, Rosenbaum DS. Europace 2007; 9: vi77-vi82.

Methods

Overview:

Figure 5 shows an overview of the methods used to test our hypotheses. First, EMS patients included in the study were sorted into one of three outcome groups (classes): no rearrest, PEA rearrest, and VT/VF rearrest. ECGs were then annotated and processed, after which RR variability and repolarization variability features were calculated. All features and their respective outcome groups are assembled for machine learning. After feature selection and CV settings are determined, a linear support vector machine (SVM) is trained using the feature data and respective class labels. The median performance metrics from 5 iterations of classification were reported. Further details regarding each step are reported in the following sections.

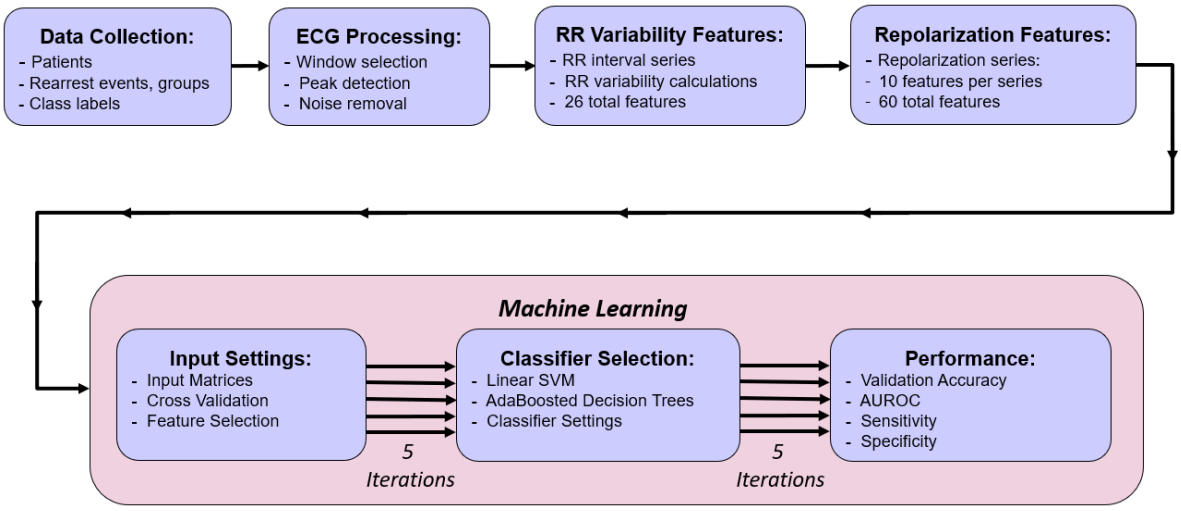

Figure 5: An overview of the methods for using RR variability and repolarization features derived from the ECG to predict cardiac rearrest occurrence and mechanism.

Data Collection:

This study was approved by the MetroHealth System Institutional Review Board. Three hundred thirty-eight Cleveland EMS patients who experienced an out of hospital cardiac arrest and were treated at MetroHealth Medical Center between January 1, 2018, through December 31st, 2022, were screened for inclusion in this study. Only patients who had ROSC were included. Patients including children <18, prisoners, and pregnant women were excluded. Additionally, patients with unconfirmed rearrest rhythms, or missing/illegible ECG signals were excluded. The remaining 87 individual patients with 94 ECGs (some had multiple rearrests) were

analyzed. ECG rhythm strips were initially reviewed with *Zoll RescueNet Code Review* software. The times of ROSC and rearrest were identified, along with rearrest rhythms. Of the 94 ECGs, 48 had no rearrest, 30 had a rearrest due to PEA and 16 had a pulseless VT or VF rearrest. From each ECG, a period after ROSC with minimal noise was selected for further analysis. Importantly, because we were interested in predicting rearrest, the analysis period was selected to be as close as possible to the rearrest event. In patients that did not rearrest, a similar time after ROSC was chosen.

ECG Processing:

ECG traces were first uploaded into custom software that allows users to view and annotate signals. When available, a 2-minute window beginning after ROSC from primary arrest was selected for analysis. Window selection was based on the 2-minute window used in a similar study (*Elola et al*) who used RR variability to predict occurrence of rearrest[19]. Otherwise, the largest available window was used. Of the 94 ECGs, 55% had the desired 2-minute window and 86% had at least a 1-minute window. For each beat in the ECG, 3 time points were automatically annotated and manually verified for subsequent interval analysis and removal of baseline wander: the R-wave peak, T-wave peak, and mid-PQ isoelectric point. The PQ interval was

chosen over the more common TP interval because it was more reliably present in the post-cardiac arrest setting. Figure 6 shows example annotations on a single beat from a representative ECG.

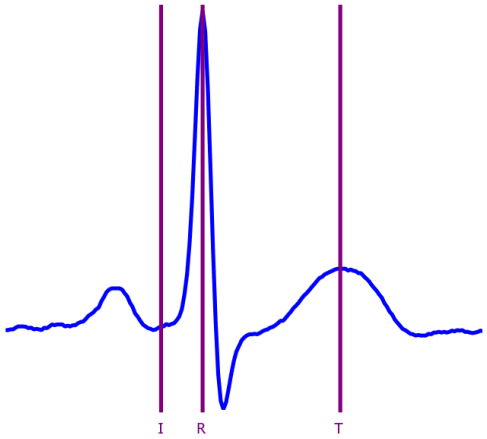

Figure 6: Annotations (purple lines) identifying the indices of the mid-PQ isoelectric (I) point, R-wave (R) and T-wave (T) peaks on a sample beat from a representative ECG.

After annotation, ECGs were then processed to remove high and low frequency noise using MATLAB. First, high frequency noise was filtered out using a low-pass digital filter. A Butterworth filter was selected for its maximally flat behavior in the passband and the lack of rippling typically observed in the passband or stopband of Chebyshev and Elliptic filters. A filter order of 5 and a cutoff frequency of 30 Hz was chosen for the filter design. Figure 7 shows a sample ECG with high frequency noise,

before and after low-pass filtering. A cubic spline was fitted to the mid-PQ isoelectric points with a sampling frequency equal to the ECG (250 Hz). This isoelectric spline served as an estimate of baseline wander and was subtracted from the ECG to remove low frequency noise. The method of subtracting an isoelectric spline was adopted from *Nearing et al*, who used the same method prior to analysis of TWA[27]. Figure 8 shows a sample ECG with baseline wander, before and after subtraction of the isoelectric spline.

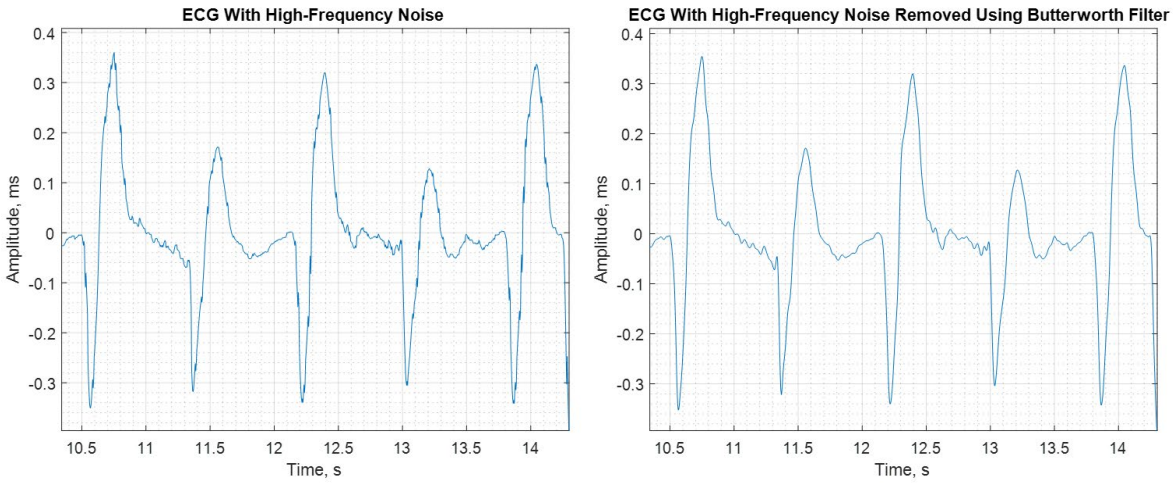

Figure 7: Original ECG with high frequency noise (left) and after low-pass filtering (right).

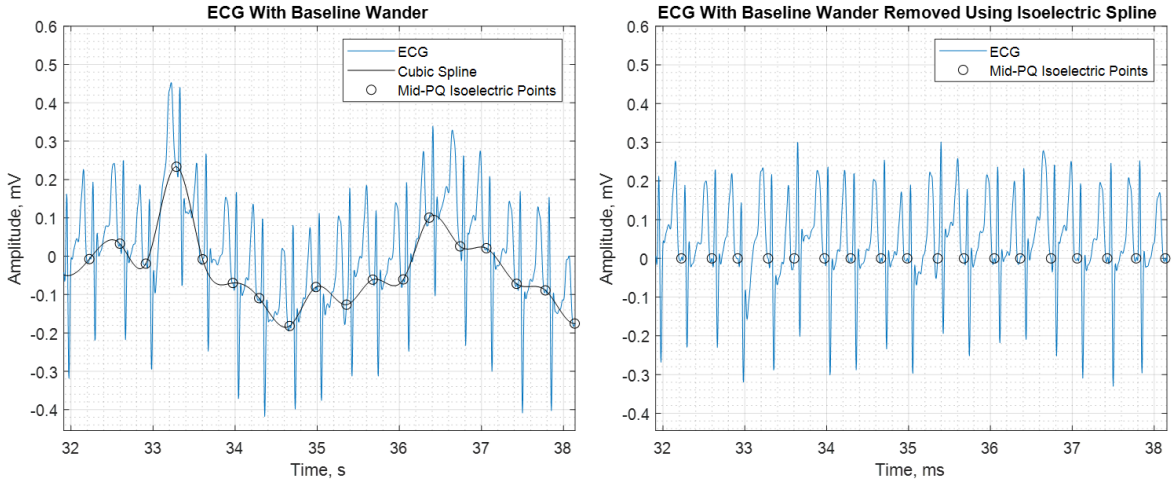

Figure 8: Original ECG (left, blue) with baseline wander estimated by a cubic spline (black) fit to mid-PQ isoelectric points and after removal by subtracting the spline (right).

Calculation of RR Variability Features for ML:

The RR interval was calculated as the time difference between successive R-wave peaks for every beat in an ECG trace (RR interval series). Figure 9 shows the beat level measurement made on a representative ECG that constitutes the RR interval series. For a total of N analyzed beats, the RR interval series is $N - 1$ in length. Figure 10 shows a sample RR interval series.

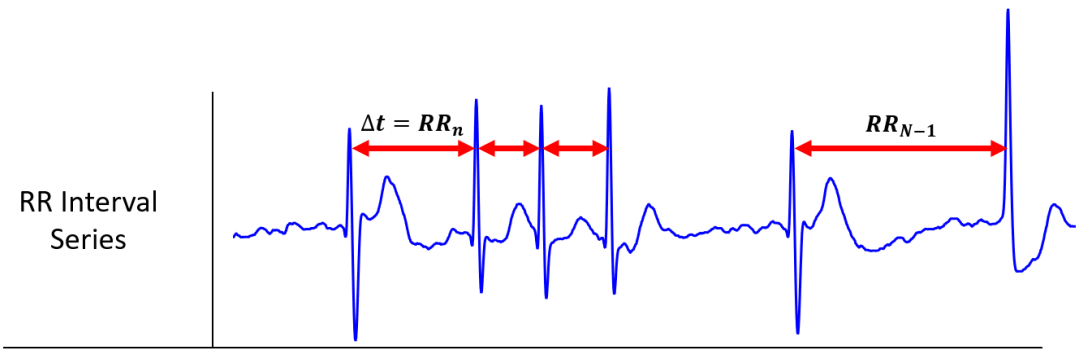

Figure 9: The RR interval series (red bidirectional arrow) on a representative ECG.

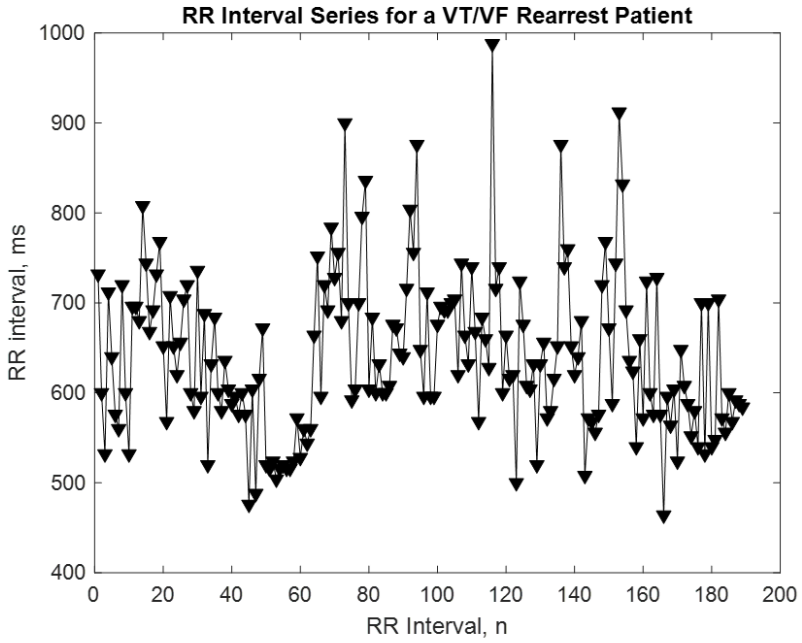

Figure 10: RR Interval series taken from the period of ROSC for a patient who had a VT/VF rearrest.

From the RR interval series, multiple measures of variability were calculated as features to use in ML. Metrics typically used to measure heart rate variability for clinical testing were borrowed for this purpose. These features were calculated according to the standards defined by the Task Force of The European Society of Cardiology and The North American Society of Pacing and Electrophysiology[13] and were grouped as described below. The Task force recommends that HRV is calculated on ECGs in normal sinus rhythm, free of ectopic beats, over a sufficient time window; recommendations that many of the ECGs used in this study do not satisfy. To acknowledge these differences, the effects they may have on our results, and the potentially different mechanisms compared to traditional HRV, we refer to HRV as RR variability in the context of this study.

Time Domain Features:

Time domain features include descriptive statistics and geometric methods that describe the histogram shape of the RR interval series. Descriptive statistics included measures of beat-to-beat and overall variance and measures of central tendency.

Frequency Domain Features:

For frequency domain features, resampling of the RR interval series was necessary for estimation of the periodogram from which all frequency domain features are calculated. The RR interval series was resampled by interpolation with a cubic spline. A Welch periodogram with a Hann window was then used to estimate the power spectral density of the interpolated RR interval series and calculate the frequency domain features. Figure 11 shows the ECG, resampled RR interval series, and resulting periodogram for a patient who had a PEA rearrest. Low and high frequency bands are shaded in blue and red, respectively. All traditional frequency domain features were used except those belonging to the ultra-low frequency range. This period of recording was excluded because a very long recording time of 24 hours is recommended[13,14].

Non-linear Features:

The Poincaré plot of the RR interval series was necessary for the calculation of 4 non-linear features, including SD1, SD2, SD1/SD2, and ellipse area. To create the plot, each RR interval was plotted against its successive interval. SD1 measures the standard deviation of points along the line perpendicular to the line of identity. SD2 measures the standard deviation of points along the line of identity. The ellipse is

measured as $\pi * SD1 * SD2$. These features are intended to measure short term and long term variability[14]. Figure 12 shows a sample Poincaré plot for two patients: one who did not rearrest, and one who had a PEA rearrest. The respective lines along which SD1 and SD2 are measured are also shown in Figure 12. The other two non-linear features are approximate entropy and sample entropy. Two algorithms were developed for approximate and sample entropy with guidance from *Delgado-Bonal et al*[42]. Exact replica examples from their study were utilized and tested on both algorithms. Trivial examples including vectors with either zero variability or various repeating patterns were also tested. Algorithms were accepted for implementation when the outputs exactly matched those reported in *Delgado-Bonal et al*[42]. Entropy measures predictability by assessing how "similar" points are relative to each other in N dimensional space. Similarity is quantified by comparing the pointwise distance between subsequences of the RR interval series. The total number of similar patterns within a specified tolerance level are counted and then used to calculate approximate or sample entropy[42]. The size of the subsequence vectors was set to 2, and the tolerance level was set to 0.2 times the standard deviation of the RR interval series. It is important to note that sample entropy and approximate entropy are very similar measures of predictability. However, approximate entropy has a self-counting bias

when considering the total number of similar patterns between subspaces, because it will compare a subspace with itself. This results in the RR interval series being more predictable, and having lower entropy, than it would without the self-counting bias. Detrended fluctuation analysis was excluded in this study because it was designed to measure recordings that are hours long in duration[14].

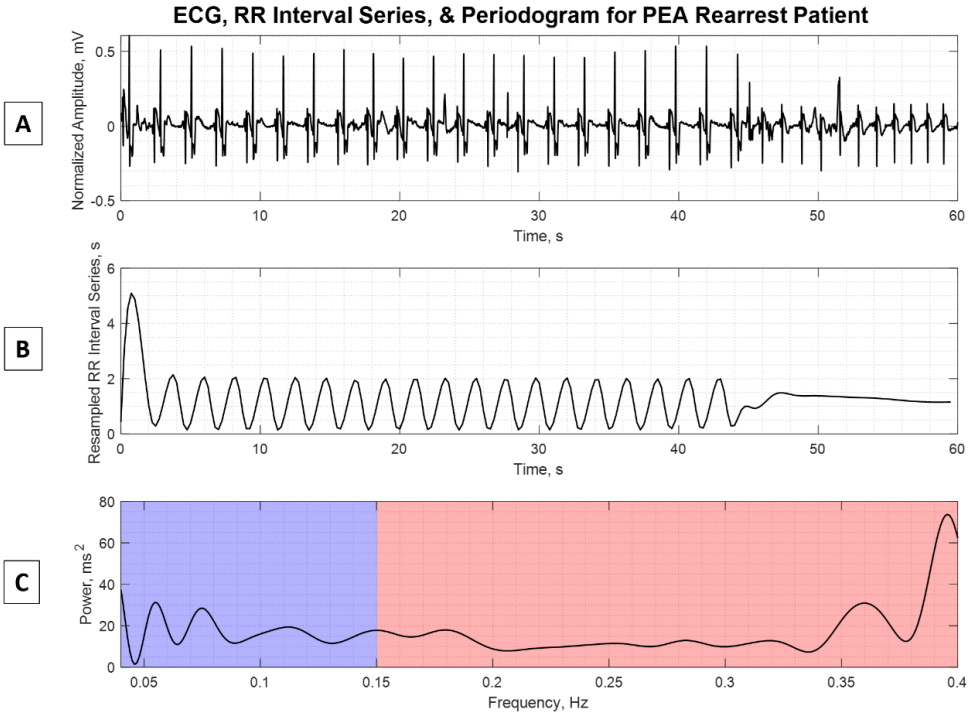

Figure 11: Panel A – Normalized ECG from a patient with bigeminy who had a PEA rearrest. Panel B – Resampled RR interval series. The short-long-short pattern from bigeminy is apparent. Panel C – The resulting Welch periodogram over the traditional physiologic range. The blue shaded region indicates the low frequency band, while red indicates the high frequency band.

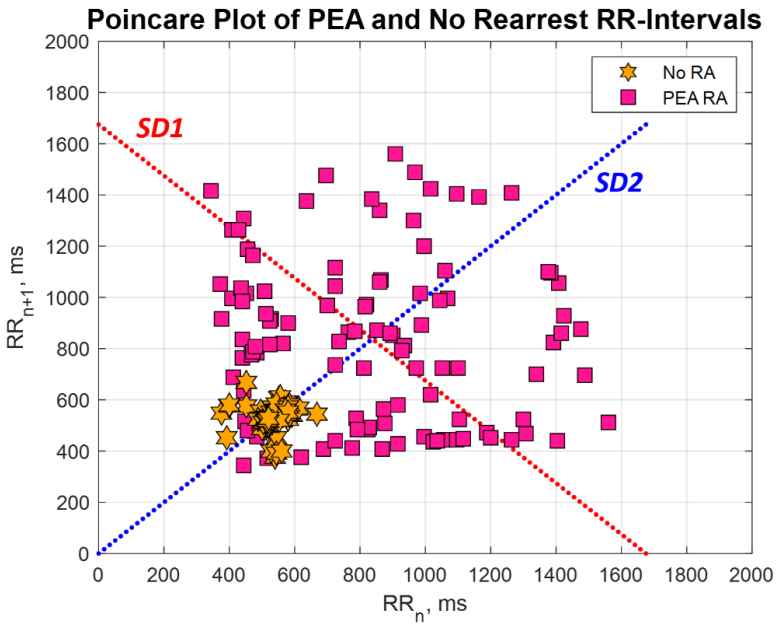

Figure 12: A Poincaré plot for a patient who did not rearrest (yellow stars) and a patient who had a PEA rearrest (pink squares). Feature SD1 measures variability along the red dotted line while feature SD2 measures variability along the blue dotted line.

Calculation of Repolarization Variability Features for ML:

Repolarization variability features were calculated from repolarization time series constructed using T-wave peak annotations including T-wave amplitude, QT interval, and repolarization area, similar to that for the RR interval. The peak T-wave amplitude of each beat was extracted from the ECG using the T-wave annotation indices identified previously. The time of R-wave and T-wave peaks was extracted using the R-wave and T-wave peak annotation indices, the sampling rate, and the number of elements or points in the ECG. T-wave peak amplitude was measured as

voltage (mV) relative to the mid-PQ isoelectric point. The QT interval was measured as the time from the R-wave peak to the T-wave peak, in seconds. This measurement is approximate since, clinically, the QT interval is measured from the beginning of the of the QRS complex to the end of the T-wave. The repolarization area was calculated as the product of the QT interval and the T-wave peak amplitude and measured in millivolt-seconds. Figure 13 shows the beat-level measurements that comprise each time series and Figure 14 shows a sample T-wave amplitude series. Ten applicable features from RR variability were adopted, including time domain and non-linear features that measure the predictability of the repolarization series'. Sample entropy was used exclusively as the measure of series predictability. Approximate entropy was excluded because of the self-counting bias explained above.

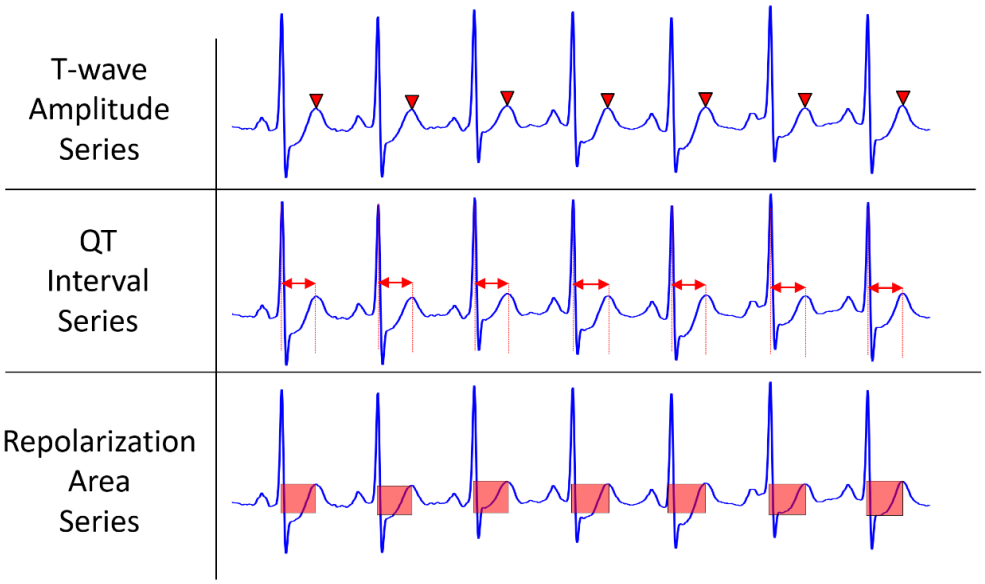

Figure 13: Beat level measurements that constitute the T-wave amplitude, QT interval and repolarization area series.'

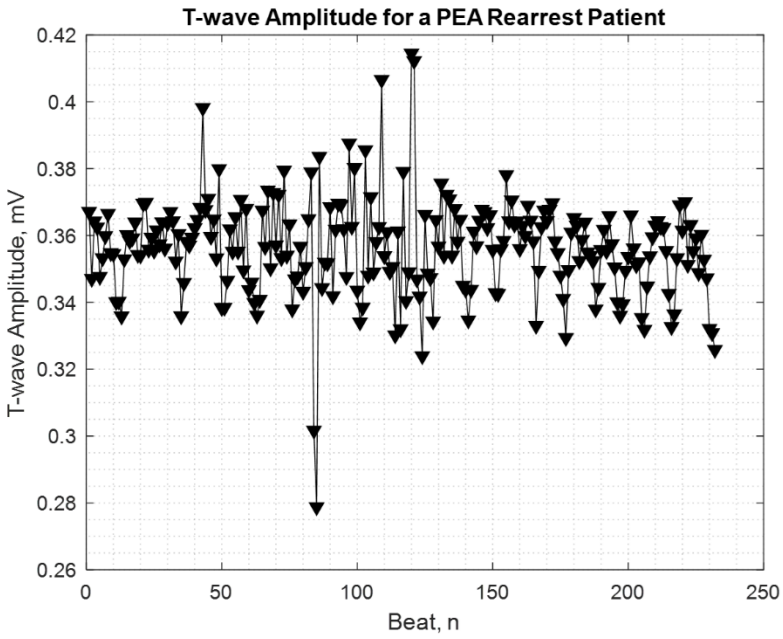

Figure 14: T-wave amplitude series from a representative 2-minute ECG trace.

Given that the RR variability features we borrowed do not describe T-wave oscillating patterns that have been previously associated with cardiac pathology, we calculated a beat-by-beat measure of T-wave amplitude oscillations. TWA (2:1), and T-wave amplitude oscillations (3:1 and 4:1) were calculated from the T-wave amplitude series described above (resulting in a series of a series). The oscillation amplitude of the T-wave at frequencies of 1/2, 1/3, and 1/4 was extracted by complex demodulation of the T-wave amplitude series to construct a new series that describes beat-by-beat T-wave oscillations. Complex demodulation is an analysis

technique that similar studies have used to provide a continuous measure of the magnitude of T-wave oscillations at different frequencies[25,27,43,44]. This method of analysis is advantageous because it requires less than 30 seconds of ECG trace, is tolerant of stationarity changes, and is resistant to phase shifts[43,44]. Complex demodulation of the T-wave will therefore provide a beat-by-beat measure of the oscillation amplitude at any specified frequency of interest. First, the T-wave amplitude series was extended on both ends to eliminate an undesirable edge effect that appears when filtering the demodulated signal. This was done by reflecting a portion of the T-wave amplitude series at both end points. The demodulating function was defined as a cosine waveform with a frequency equal to the oscillation frequency of interest (1/2, 1/3, or 1/4). Next, the T-wave amplitude series was multiplied by the demodulating function. A low-pass Butterworth filter was used to isolate the time varying oscillation amplitude at the frequency of interest using a filter order of 6 and cutoff frequency of 0.183π, as used by *Nearing et al*[44]. After filtering, the extended signal portions containing the edge effect are removed, and the demodulated signal is restored to its original size. Figure 15 shows the resulting time varying amplitude series, $a(t)$, for a simulated ECG with transient TWA after complex demodulation. The same ten features from RR variability used on the other repolarization series'

described above were calculated on the T-wave amplitude oscillation series'. These include 5 time domain and 5 non-linear features. Figure 16 shows beat-level sample measurements made on representative ECGs for each of the T-wave amplitude oscillation series.

In summary, a total of 60 repolarization features were calculated for machine learning (10 from each of the six series'). Table 1 lists all features and identifies those applied to the six repolarization series'. Equations used to calculate each feature can be found in Tables 2-4.

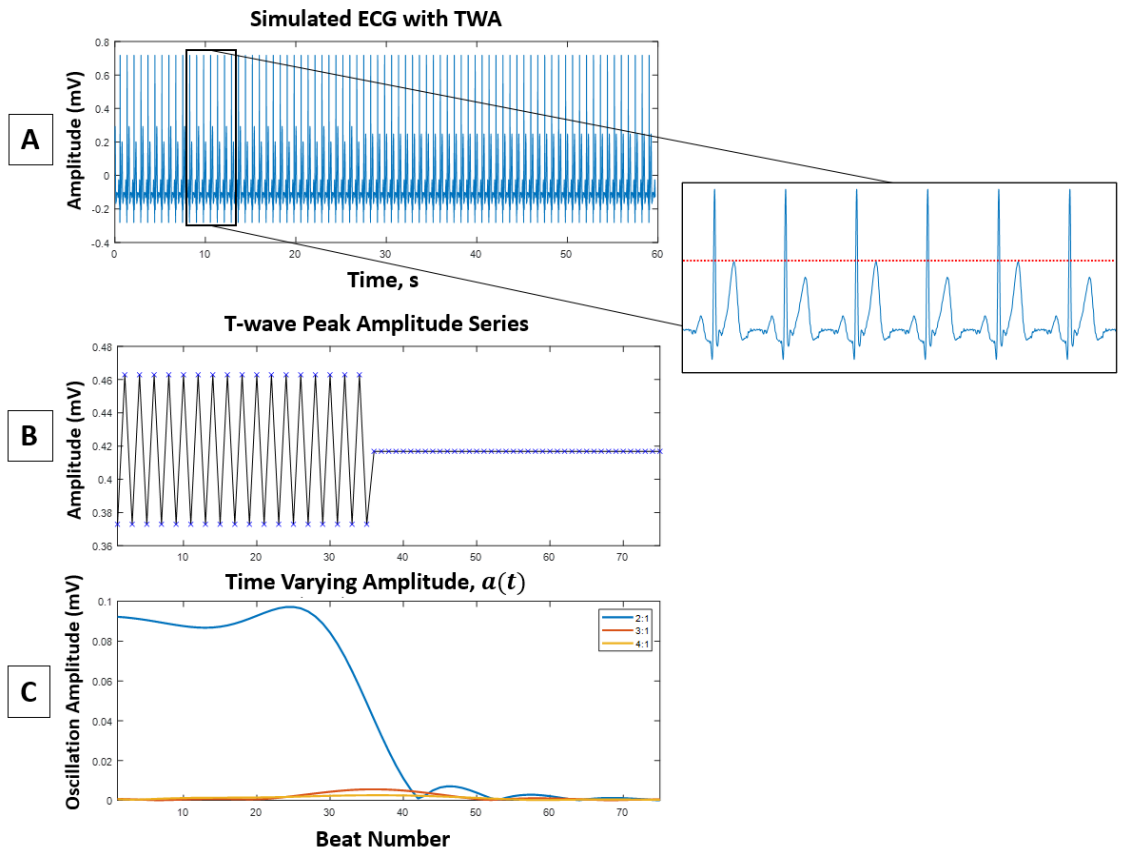

Figure 15: Panel A – Simulated ECG with TWA present in the first half and no amplitude oscillations present in the second half. Panel B – The T-wave amplitude series. Panel C – The time varying amplitude series, a(t), after complex demodulation of the T-wave.

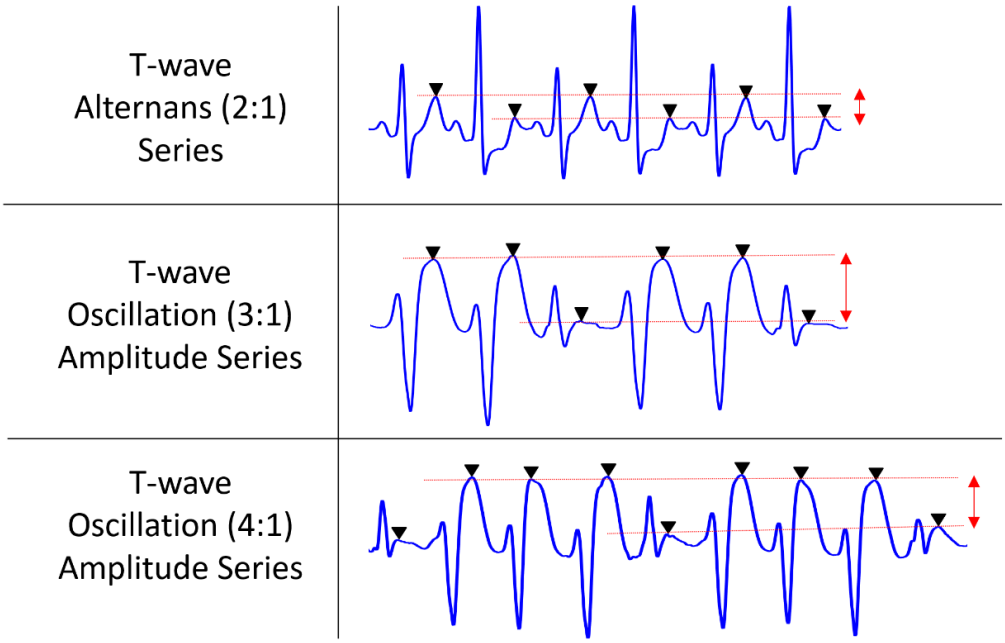

Figure 16: T-wave amplitude oscillations at frequencies of every other beat or 1/2 (top), every third beat or 1/3 (middle), and every fourth beat or 1/4 (bottom). Oscillation amplitude is represented by the red bidirectional arrows.

	Feature Number	Feature	Repolarization Series'	RR Interval Series
Time Domain	1	Standard Deviation	**X**	**X**
	2	Average	**X**	**X**
	3	pNN50		**X**
	4	RMSSD		**X**
	5	Minimum Value	**X**	**X**
	6	Maximum Value	**X**	**X**
	7	Range	**X**	**X**
	8	Triangular Index		**X**
	9	TINN		**X**
Frequency Domain	10	VLF Abs. Power		**X**
	11	VLF Peak Frequency		**X**
	12	LF Abs. Power		**X**
	13	LF Peak Frequency		**X**
	14	HF Abs. Power		**X**
	15	HF Peak Frequency		**X**
	16	LF:HF Ratio		**X**
	17	Total Abs. Power		**X**
	18	VLF Relative Power		**X**
	19	LF Relative Power		**X**
	20	HF Relative Power		**X**
Non-Linear	21	SD1	**X**	**X**
	22	SD2	**X**	**X**
	23	SD1:SD2 Ratio	**X**	**X**
	24	Ellipse Area	**X**	**X**
	25	Approximate Entropy		**X**
	26	Sample Entropy	**X**	**X**
Total Features (# of series x # features)			**60**	**26**

Table 1: List of features measured on RR interval and repolarization series.

Time Domain	Standard Deviation (SDRR), ms	$\sqrt{\frac{1}{N}\sum_{i=1}^{N}(x_i - \mu_i)^2}$
	Average, ms	$\frac{1}{N}\sum_{i=1}^{N} x_i$
	pNN50, %	Given $X = (x_{2:N} - x_{1:N-1}),\ pNN50 = \left[\frac{card(X \geq 50)}{card(X)}\right] * 100$
	RMSSD, ms	$\sqrt{\frac{1}{N}\sum_{i=1}^{N-2}(x_{i+1} - x_i)^2}$
	Minimum Value, ms	Given $X = \{x_1, x_2, \ldots x_N\},\ X_{Min} = \min(X)$
	Maximum Value, ms	Given $X = \{x_1, x_2, \ldots x_N\},\ X_{Max} = \max(X)$
	Range, ms	$(X_{Max} - X_{Min})$
	Triangular Index	Given $X = \{x_1, x_2, \ldots x_N\},\ Triangular\ Idx. = \frac{card(X)}{card(modal(X))}$
	TINN, ms	Given x as the smoothed histogram of input series and x_{peak} as the maximum frequency, $M = first(x > x_{peak} == 0), N = last(x < x_{peak} == 0)$ $TINN = M - N$

Table 2: Equations for time domain features measured on RR interval and repolarization series.

Frequency Domain	VLF Absolute Power, ms²	Given periodogram S_w with discrete frequencies f, $VLF = \frac{S_{w,f=0} - S_{w,f=0.04}}{2N} \sum_{i=1}^{N} \left(S_w(f_i) + S_w(f_{i+1})\right)$
	VLF Peak Frequency, Hz	Given periodogram S_w, $VLF\ Peak\ freq. = f_{Max(S_w, 0 \leq f \leq 0.04)}$
	LF Absolute Power, ms²	Given periodogram S_w with discrete frequencies f, $LF = \frac{S_{w,f=0.04} - S_{w,f=0.15}}{2N} \sum_{i=1}^{N} \left(S_w(f_i) + S_w(f_{i+1})\right)$
	LF Peak Frequency, Hz	Given periodogram S_w, $LF\ Peak\ freq. = f_{Max(S_w, 0.04 < f \leq 0.015)}$
	HF Absolute Power, ms²	Given periodogram S_w with discrete frequencies f, $HF = \frac{S_{w,f=0.15} - S_{w,f=0.4}}{2N} \sum_{i=1}^{N} \left(S_w(f_i) + S_w(f_{i+1})\right)$
	HF Peak Frequency, Hz	Given periodogram S_w, $HF\ Peak\ freq. = f_{Max(S_w, 0.15 < f \leq 0.4)}$
	Ratio (LF/HF)	$\frac{LF}{HF}$
	Total Absolute Power, ms²	$VLF + LF + HF$
	VLF Relative Power	$\frac{LF}{VLF + LF + HF}$
	LF Relative Power	$\frac{VLF}{VLF + LF + HF}$
	HF Relative Power	$\frac{HF}{VLF + LF + HF}$

Table 3: Equations for frequency domain features measured on the RR interval series.

Non-Linear	SD1, ms	$\sqrt{\frac{1}{N-1}\sum_{i=1}^{N-1}\left(\frac{x_{i+1}-x_i}{\sqrt{2}}\right)^2}$
	SD2, ms	$\sqrt{\frac{1}{N-1}\sum_{i=1}^{N-1}\left(\frac{x_{i+1}+x_i}{\sqrt{2}}\right)^2}$
	SD Ratio	$\frac{SD1}{SD2}$
	Ellipse Area, ms^2	$C_n = \pi * SD1 * SD2$
	ApEn	$-\frac{1}{N-m}\sum_{i=1}^{N-m}\log(\frac{\sum_{j=1}^{N-m}[card(\lvert x_{m+1}(j)-x_{m+1}(i)\rvert < r\sigma(RR))]}{\sum_{j=1}^{N-m}[card(\lvert x_m(j)-x_m(i)\rvert < r\sigma(RR))]}$
	SampEn	$-\log(\frac{\sum_{i=1}^{N-m}\sum_{j=1,i\neq j}^{N-m}[card(\lvert x_{m+1}(j)-x_{m+1}(i)\rvert < r\sigma(RR))]}{\sum_{i=1}^{N-m}\sum_{j=1,j\neq i}^{N-m}[card(\lvert x_m(j)-x_m(i)\rvert < r\sigma(RR))]}$

Table 4: Equations for non-linear features measured on RR interval and repolarization series.

Input Data and Cross Validation Settings:

To predict rearrest occurrence and type, ML was used in MATLAB's Classification Learner App (software version 2022b). Class labels were assigned to all 94 ECGs. For prediction of rearrest occurrence (a binary response) class labels "no rearrest" and "rearrest" were used. In this case, patients who really had a PEA or VT/VF rearrest were simply labeled as having a "rearrest." For prediction of rearrest type (a multiclass response) class labels "no rearrest," "PEA rearrest," and "VT/VF rearrest" were used. Features and their corresponding class labels were assembled

into a matrix consisting of $\boldsymbol{p}$ columns of features (depending on the number of features used) and a class label for all 94 ECGs, resulting in a matrix of size [94 x $\boldsymbol{p}$].

For cross validation, K-fold stratified and unseeded CV was used to partition the data into training and testing sets using $k = 10$ folds. The fold value $k = 10$ was chosen over $k = 5$ to increase the partition of data in the training set. Stratified CV ensures that class representation in each fold is proportionate to class representation in the whole dataset. This was necessary to ensure that the minority VT/VF rearrest class, which had only 16 events, was well represented in each fold. For 10-folds, this was approximately 1.6 VT/VF patients per fold. Unseeded cross-validation was specified to allow variability in the partitioning of data to each of the 10-folds. If a seed state were specified, the same events would be assigned to the same folds whenever data was trained on the classifier. Allowing variation in the assignment of data to different folds offered a more balanced view of classifier performance. In conjunction with unseeded CV, each classification problem was analyzed 5 separate times to estimate the degree of variability in classifier performance with different CV partitions.

In order to determine whether models were affected by overfitting, we performed analyses with and without feature selection. A simple filter method was used for feature selection, which ranked Analysis of Variance (ANOVA) p-values on a transformed negative logarithm scale. The transformation scaled and emphasized the p-value significance. When feature selection was used, the top 25 features were chosen for use in the ML models. In this study, feature importance is determined by the value of the ANOVA rank from feature selection, where the feature with the smallest p-value and therefore the highest rank is considered the most important.

Classifier Selection Options:

In preliminary testing of both the binary response (no rearrest vs. rearrest) and multiclass response (no rearrest vs. PEA rearrest vs. VT/VF rearrest), support vector machines (SVM) and ensemble methods (bagged or boosted decision trees), performed comparably well. In addition to its relatively high preliminary performance, the linear SVM was ultimately selected for its popularity, flexibility, effectiveness in high dimensional spaces, and robustness to overfitting[45]. To optimize model performance, the box constraint parameter that determines where the dividing hyperplane lies, was optimized. Tuning the box constraint parameter allows the

model to find a balance between achieving a large margin (the hyperplane that is farthest from training data) and minimizing misclassification error[45]. Optimization was enabled to give the classifier the flexibility to find its best operating point for a given input matrix and CV partition. For multiclass response, a "one-vs-one" classification method was used, which uses majority voting on multiple binary models to classify observations[45].

For direct comparison to a similar study by *Elola et al*[19], we used MATLAB's ensemble classifiers – bootstrap aggregated, or bagged, decision trees and adaptive boosted decision trees. It is worth noting that RF, bagged, and boosted decision trees are very similar tree-based ensemble methods that use numerous weak learners, or shallow trees, to make predictions. Higher preliminary performance led to the selection of adaptive boosted (Adaboost) decision trees for comparison to *Elola et al's* RF classifier. Three tuning parameters were left unassigned for optimization: the maximum number of tree splits, number of weak learners, and learning rate. These tuning parameters are optimized in parallel to find a balance between generalizability and complexity of the model. As before, optimization was enabled to identify the classifier's best operating point for a given input matrix and CV partition.

Machine Learning Models:

We analyzed a total of six machine learning models. They are summarized in Table 5 below. First, we used RR variability features to predict rearrest occurrence using a linear SVM and an AdaBoosted decision tree. We next used all features to predict rearrest occurrence using a linear SVM both without and with feature selection. We then used RR variability metrics to predict rearrest type using a linear SVM. Next, all features were used to predict rearrest type using a linear SVM with feature selection. When only RR variability features were used, the number of input features, $\boldsymbol{p}$, was 27 (26 features +1 column for class labels). If all features were used, $\boldsymbol{p}$ was 87 (86 features + 1 column for class labels).

Model Type	***Feature Set***	***Feature Selection***	***Response***
Linear SVM	RR	No	Rearrest Occurrence
AdaBoost Decision Trees	RR	No	Rearrest Occurrence
Linear SVM	RR & Repolarization	No	Rearrest Occurrence
Linear SVM	RR & Repolarization	Yes	Rearrest Occurrence
Linear SVM	RR & Repolarization	Yes	Rearrest Type

Table 5: Summary of the five machine learning problems we addressed in this study. We varied the model type, feature set, the use of feature selection and the response type to address the research question.

Performance Metrics Chosen:

Six metrics were selected to assess the performance of the classifiers including area under the receiver operating curve (AUROC), sensitivity, specificity, and validation accuracy. All performance metrics were chosen at the model's optimized operating point. The median performance value for each metric from 5 classification iterations was reported.

Results

Patient Population Characteristics:

ECG characteristics, patient demographics and arrest characteristics were compared using one-way ANOVA or Chi-Square statistical tests and are shown by rearrest type/group in Table 5. The ECG characteristics, ECG analysis window length and number of beats per analysis window were not statistically different between the three groups. Moreover, the groups were well matched regarding both demographics and arrest characteristics, suggesting that these patient-level differences alone cannot be predictors of rearrest occurrence or type. This patient population had demographic and arrest characteristics that are similar to other studies of CA/rearrest[46-50].

Metric	No RA	PEA RA	VT/VF RA	p-value
ECG Characteristics				
Window length (seconds)	100 ± 32	105 ± 40	98 ± 70	0.83
Number of beats analyzed	175 ± 66	164 ± 74	173 ± 127	0.85
Demographics				
Age	52 ± 14	59 ± 12	60 ± 8	0.07
Sex (% Male)	61%	61%	45%	0.63
Race (% White)	72%	64%	64%	0.75
Ethnicity (% Hispanic)	17%	19%	9%	0.75
Arrest Characteristics				
Bystander CPR	57%	54%	45%	0.80
AED use	22%	39%	27%	0.27
Time from arrest to initial ROSC (min)	20 ± 12	22 ± 11	14 ± 10	0.18
Epinephrine	72%	93%	82%	0.09

Table 6: ECG characteristics, demographics, and arrest characteristics by rearrest type. The groups are well matched, and no significant differences exist.

Survival by Primary and Rearrest Rhythms:

Figure 17, Panel A shows survival rates by primary arrest type and Panel B shows survival rates by rearrest type. As shown by others, patients who had a VT/VF primary arrest rhythm were much more likely to survive than those who had asystole or PEA ($p<0.004$, $p<0.002$)[46-48,51]. Similarly, patients who had a VT/VF rearrest were more likely to survive than those who had a PEA rearrest ($p<0.002$). Figure 18, Panel A shows primary arrest etiology by rearrest type. Etiology is presented as two categories: cardiac vs. respiratory, which also includes, overdose, drowning, and

"other." The primary arrest etiology in the no rearrest and PEA rearrest groups were balanced between cardiac and respiratory, while the VT/VF rearrest group etiology was predominantly cardiac in nature. Figure 18, Panel B shows the number of patients with each different primary arrest type (VT/VF, PEA, asystole) in each rearrest group. For the VT/VF rearrest group, the primary arrest type was largely VT/VF. The PEA rearrest group had relatively balanced amounts of asystole, PEA, and VT/VF primary arrest types. Patient survival rates, rhythm proportions and arrest etiology are consistent with other reports of CA and rearrest[7,52]. These results suggest that our patient population is representative of the larger CA populations, such that our results are potentially generalizable and may be applied to a broader group of CA/rearrest populations.

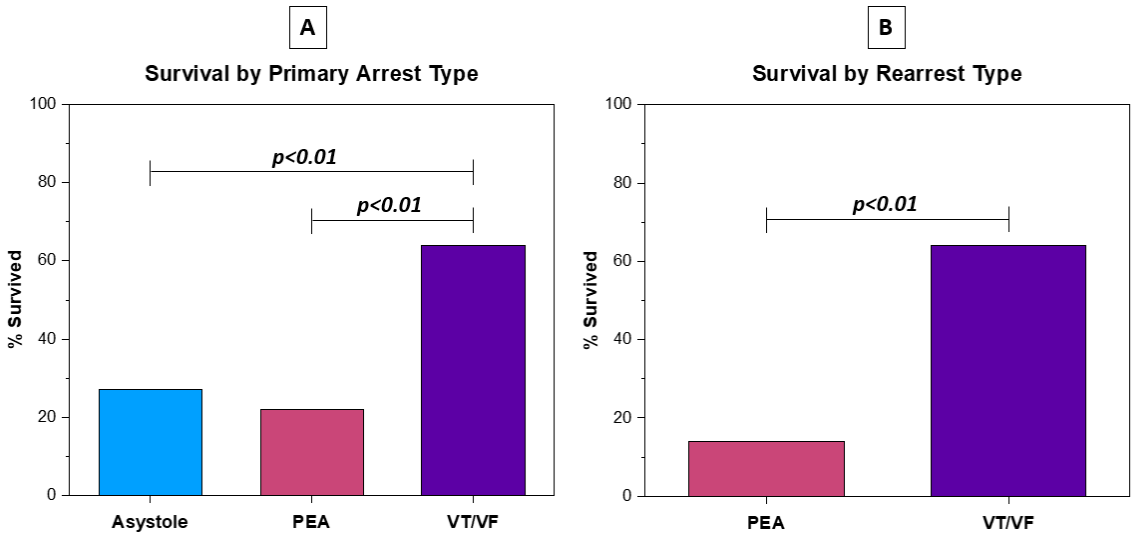

Figure 17: Panel A – Percent survival by primary arrest type. Panel B – Percent survival by rearrest type. Patients who have a VT/VF primary or rearrest type have the greatest odds of survival.

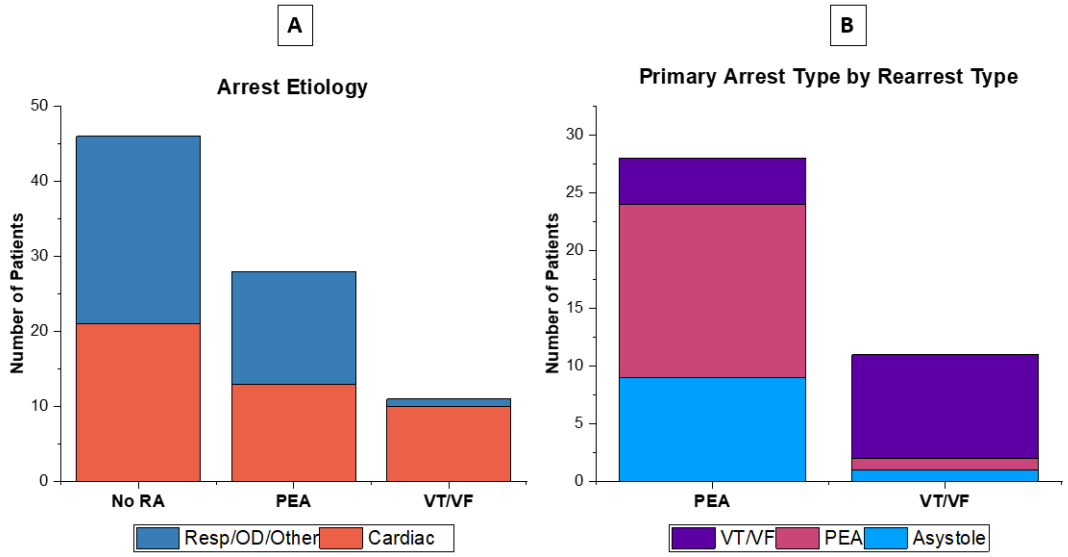

Figure 18: Panel A – Arrest Etiology by rearrest group. Etiology is analyzed as two separate groups: cardiac or respiratory, which also includes overdose, drowning, and others. Etiology was predominantly cardiac for patients who had a VT/VF rearrest. Panel B – Primary arrest type by rearrest type. Most patients who had a VT/VF rearrest had VT/VF primary arrest.

Machine Learning to Predict Rearrest Occurrence with RR Variability Features:

We first tested in our patient population if RR variability features could predict no rearrest or rearrest as described previously[19]. Twenty six RR variability features were used to predict cardiac rearrest occurrence (No RA vs. RA) using a 10-fold CV linear SVM classifier. The median area under the receiver operating curve (AUROC), sensitivity, and specificity from 5 iterations was used to assess performance (Table 7, Column 3-4). The SVM classifier had a median AUROC of 0.66, sensitivity (No RA) of 75% and specificity (No RA) of 53%. *Elola et al* similarly used RR variability features calculated from 2 minutes of post-ROSC ECG to predict rearrest in a cohort of out-of-hospital CA patients[19]. Compared to *Elola et al*, (Table 7, Column 3) our SVM classifier had a comparable AUROC (0.69 vs. 0.66), but lower specificity (67% vs. 53%.). It is possible that differences in ML models may be responsible for discrepancies between the outcomes. Although the linear SVM and RF classifiers performed comparably, the RF classifier likely had better performance because of its ability to handle non-linear relationships. To compare the datasets more fairly, we repeated the analysis using the ensemble method specified earlier (Adaptive boosted Decision Trees - AdaBDT). No other model parameters were changed (Table 7, Column 4). The AdaBDT classifier had a median AUROC of 0.69, sensitivity (No RA) of 73%, and a specificity (No RA) of 64%.

Now when compared to *Elola et al*, performance differences are absent or marginal. Figure 19 shows the ROC for the linear SVM and AdaBDT classifiers. These results suggest that classifier details account for performance discrepancies more than potential differences in patient population, CV, and number of features when comparing our results to *Elola et al*.

Model Specifications	***Elola et al***		**Current Study**		**Current Study**	
Number of Features	21 (17 RR variability)		26		26	
Feature Set	RR Variability & Signal		RR Variability		RR Variability	
Number of Patients	162 (33% RA)		94 (49% RA)		94 (49% RA)	
Cross-Validation	5		10		10	
Algorithm	Random Forest		AdaBoosted Trees		Linear SVM	
Metric Validation	Median, 100 iterations		Median, 5 iterations		Median, 5 iterations	
Classes	*No RA*	*RA*	*No RA*	*RA*	*No RA*	*RA*
AUC	**0.69**		**0.69**		**0.66**	
Sensitivity	**-**	**0.67**	**0.73**	**0.64**	**0.75**	**0.53**
Specificity	**0.67**	**-**	**0.64**	**0.73**	**0.53**	**0.75**
Validation Accuracy (%)	**-**		**66**		**64**	

Table 7: Classifier performance compared to Elola et al, who also used RR variability features calculated from the ECG to predict cardiac rearrest occurrence. Green boxes indicate similar or better performance, while red indicates worsening performance when compared to Elola et al.

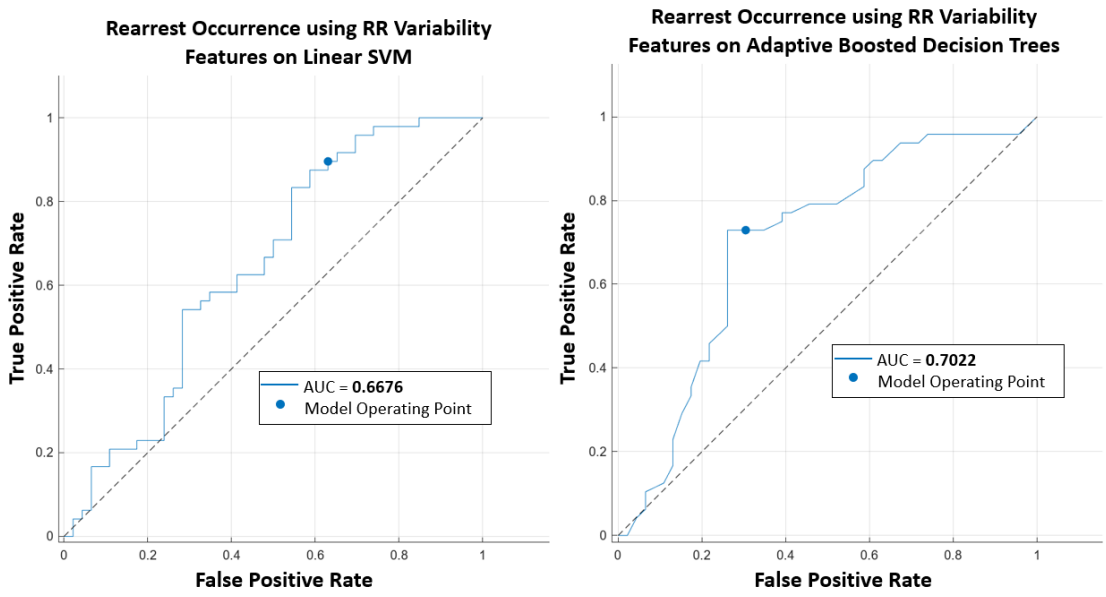

Figure 19: Receiver operating curves and model operating points for a linear SVM classifier (left) and an adaptive boosted (AdaBoost) decision tree classifier (right). Both classifiers predict cardiac rearrest occurrence using only RR variability features. The AdaBoosted decision tree model had improved performance over the linear SVM model.

Effect of Adding Repolarization Variability Features to RR Variability to Predict Rearrest Occurrence:

We hypothesized that repolarization variability features may improve the predictive capacity for rearrest occurrence, so we next evaluated whether addition of repolarization variability features affected classifier performance. The 10-fold CV linear SVM model using 26 RR variability features described in the previous section was used as the basis for comparison except that 60 repolarization variability features were combined with the RR variability features. Compared to the same

classifier with just RR variability features, performance overall was lower with decreased AUROC (0.66 to 0.64), specificity (No RA) (53% to 45%), and average validation accuracy (64% to 62%). Given the relatively poor performance of the classifier using all features (86 total), it's possible that this may be caused by overfitting. To test this, we next evaluated the model with a reduced number of input features.

Feature selection avoids overfitting by selecting a subset of features that are correlated or strongly associated with the output classes. The ranked ANOVA feature selection method was applied to the combined RR variability and repolarization variability feature set. The top 25 ANOVA ranked features were used to predict cardiac rearrest occurrence (each feature comparing no rearrest and rearrest) using the 10-fold CV linear SVM. The model using the top 25 features marginally improved performance when compared to the model using just RR variability features. Model specificity (No RA) increased (53% to 59%) and validation accuracy increased (64% to 66%) when using the top 25 features. Figure 20 shows the ROCs for representative models without and with feature selection. These models used the same input data and CV partitions but the model using the top 25 features shows improved sensitivity and AUROC (Figure 20). Figure 21 shows the confusion matrices for two

representative classifiers that use all features, and the top 25 features, respectively, to predict rearrest occurrence. The confusion matrices show how applying feature selection improved the true positive rate for the rearrest class by over 10%. These results suggest that the previous model using all features (86 total) was overfit.

Identification of the top 25 features allows us to determine which features were most statistically significant and likely important in predicting cardiac rearrest (Figure 22). Repolarization features comprised 44% of the top 25 features, with sample entropy of the QT interval being the top ranked and most important ANOVA ranked feature. Of the repolarization features in the top 25 overall, 64% were non-linear, of which 57% were measures of entropy. Additionally, measures of entropy comprise nearly a quarter of the top 25 features (24%). The distribution of time, frequency, and non-linear features among the top 25 is 36%, 16%, and 48%, respectively. These results suggest that repolarization variability features, and measures of entropy in particular, are important to successful prediction of rearrest occurrence.

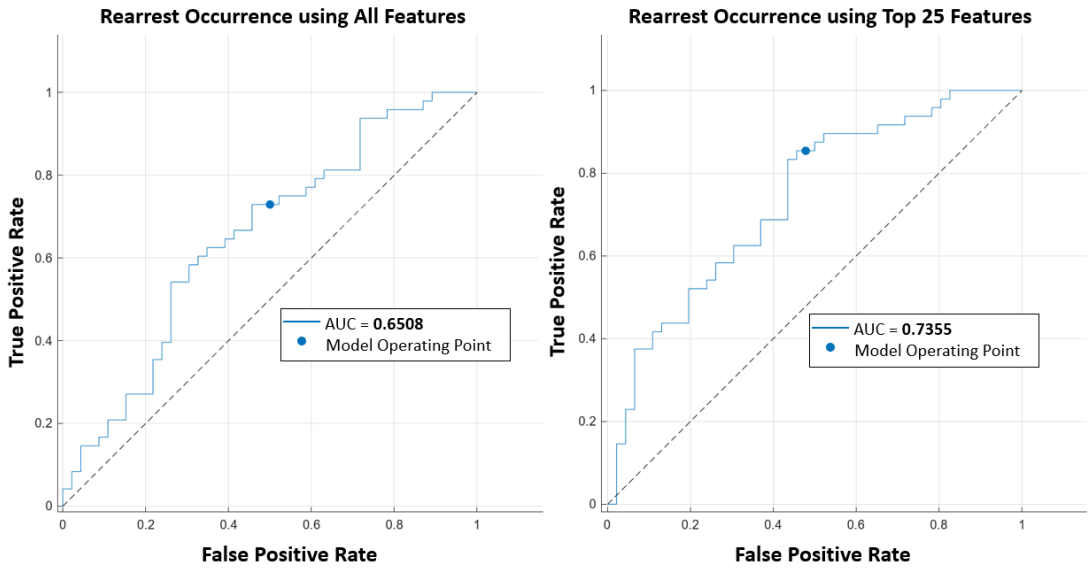

Figure 20: Receiver operating curves for the linear SVM models used to predict rearrest occurrence without feature selection (left) and with feature selection (right), using the top 25 ANOVA ranked features.

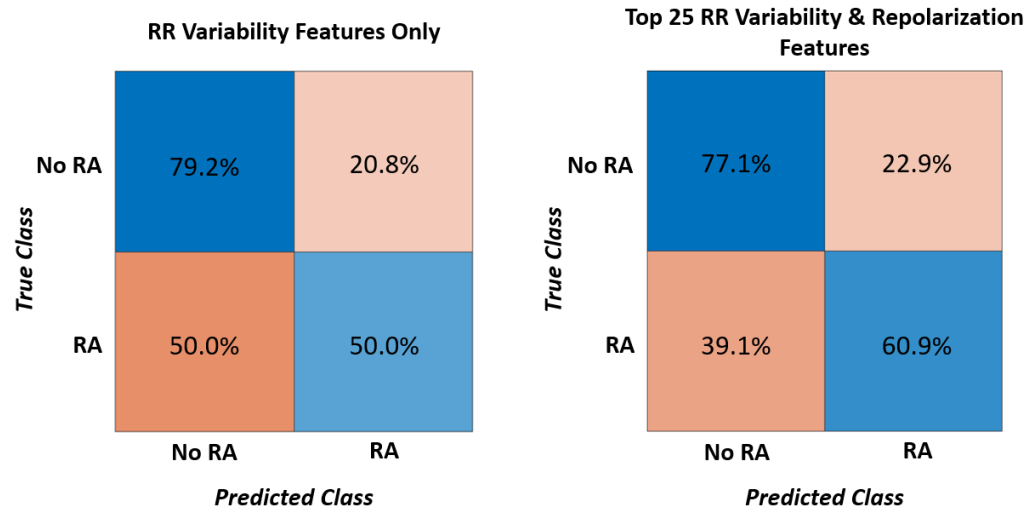

Figure 21: Representative confusion matrices for the linear SVM classifiers with RR variability features only (left) and the top 25 ANOVA ranked features (right) to predict rearrest occurrence. The true positive rate for the rearrest class improved by over10% when repolarization features were added, and feature selection was used. Hues of blue indicate true positive rates, with dark blue representing the highest true positive rate. Hues of orange represent false positive/negative rates, with dark orange representing the highest false positive/negative rate.

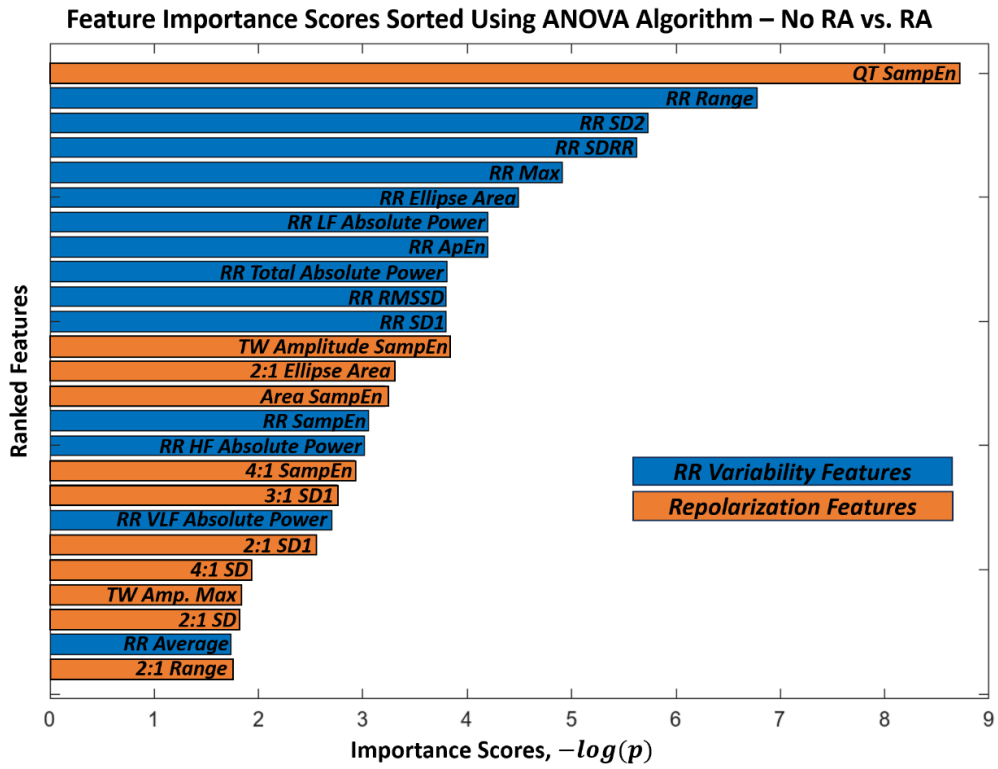

Figure 22: The top 25 features identified by the ANOVA ranking algorithm used in the Linear SVM classifier to predict cardiac rearrest occurrence. Features were selected from the combined RR variability and repolarization feature set. Repolarization features comprise 44% of the top 25. Measures of entropy comprise nearly a quarter of the top 25. The distribution of time, frequency and non-linear features is 36%, 16%, and 48%, respectively.

Effect of Adding Repolarization Features to Predict Rearrest Type:

We next evaluated whether RR variability could predict the rearrest type (i.e., PEA, VT/VF) and if the addition of repolarization variability features would improve the prediction. A 10-fold CV linear multiclass SVM using the 26 RR variability features to classify rearrest type was used as the basis for comparison. A one-vs-one method

was specified for the multiclass SVM method. From 5 iterations, the model had a median AUROC of 0.68, 0.61, and 0.61 for the No RA, PEA RA, and VT/VF RA groups, respectively (Table 8). Similarly, sensitivity was 99%, 20%, and 34% while specificity was 32%, 93%, and 92%. Finally, validation accuracy was 57%.

The model using repolarization and RR variability features did not generally improve performance when compared to the model using just RR variability features (Table 8). The only metric that improved was specificity of the VT/VF RA group. Although some performance metrics did not improve after using feature selection, they nevertheless remained high. These metrics include sensitivity of the No RA group (94%) and specificity of the PEA RA group (90%). The confusion matrices (Figure 23) show how adding the top 25 ranked features increased the true positive rate for the No RA group while also increasing false negative rates for both the PEA and VT/VF RA groups.

Identification of the top 25 ranked features from a one-way ANOVA (each feature comparing no rearrest, PEA rearrest, and VT/VF rearrest) elucidated which features were likely most important in predicting cardiac rearrest type (Figure 24). Repolarization features comprised 40% of the top 25 features, with sample entropy of

the QT interval remaining the most important ANOVA ranked feature. Measures of entropy comprise 20% of the top 25, and 40% of the top repolarization variability features. Adding repolarization features improved AUROC and specificity for the VT/VF rearrest group, however, most performance metrics remained unchanged or worsened. The distribution of time, frequency and non-linear features is 24%, 24%, and 52%, respectively. With the given classifier constraints, these results suggest that adding repolarization features to RR variability did not improve prediction of cardiac rearrest type.

Model Specifications	**RR Variability Only**			**RR Variability & Repolarization**		
Number of Features	26			Top 25		
Metric Validation	Median by 5 iterations			Median by 5 iterations		
Classes	*No RA*	*PEA*	*VT/VF*	*No RA*	*PEA*	*VT/VF*
AUC	**0.68**	**0.61**	**0.61**	**0.66**	**0.57**	**0.60**
Sensitivity	**0.99**	**0.20**	**0.34**	**0.94**	**0.20**	**0.10**
Specificity	**0.32**	**0.93**	**0.92**	**0.20**	**0.9**	**0.96**
Validation Accuracy (%)	**57**			**55**		

Table 8: Performance metrics for a 10-fold CV, multiclass, linear SVM using RR variability features, all features (RR and repolarization), and the top 25 ANOVA ranked features, respectively, to predict rearrest type. Green boxes indicate similar or better performance, while red indicates worsening performance when compared to the classifier using RR variability features only.

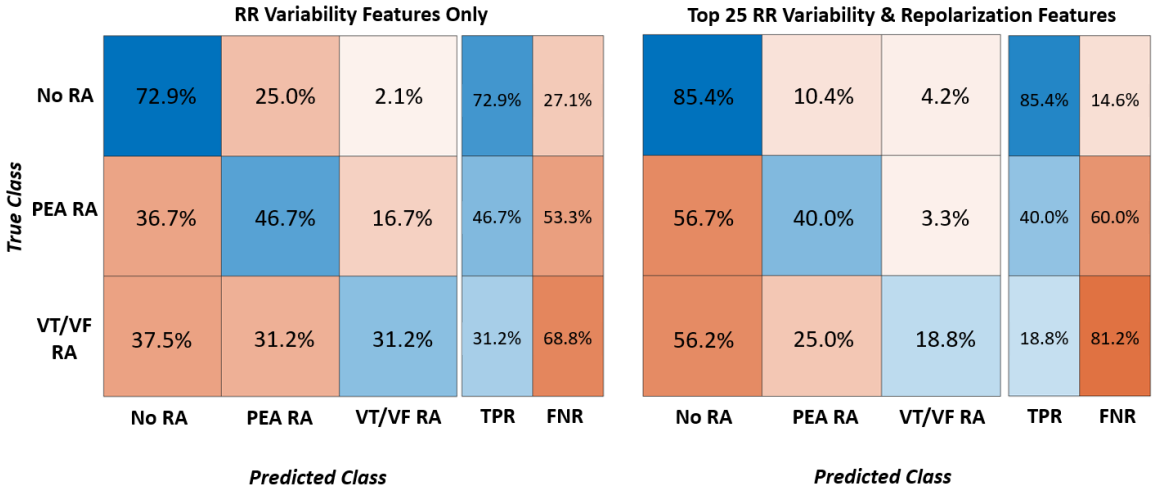

Figure 23: Representative confusion matrices for the 10-fold CV, multiclass, linear SVM classifiers using RR variability features only (left), and the top 25 ANOVA ranked features (right) to predict rearrest type. Hues of blue indicate true positive rates, with dark blue representing the highest true positive rate. Hues of orange represent false positives/negative rates, with dark orange representing the highest false positive/negative rate. The propensity of the model to classify observations as no rearrest (No RA) increases when using the top 25 ANOVA ranked features.

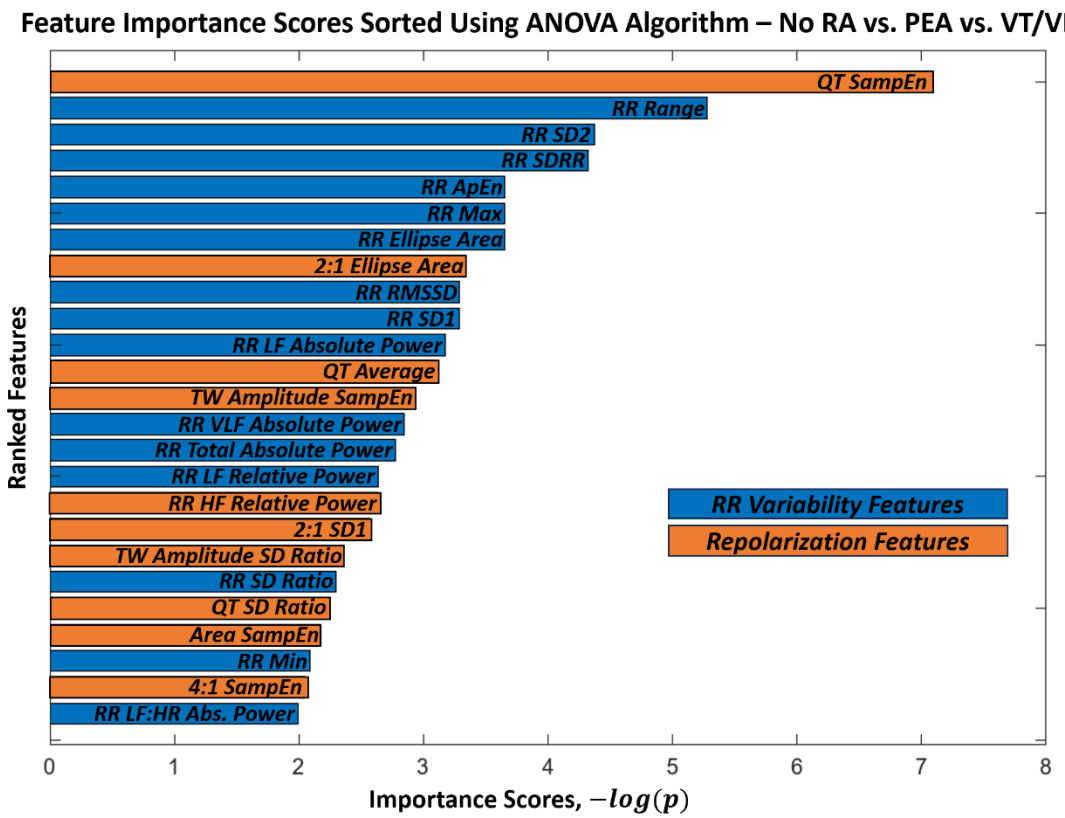

Figure 24: The top 25 most important features identified by the ANOVA ranking algorithm used in the 10-fold CV, multiclass, linear SVM. Features were selected from the combined RR variability and repolarization feature set. Repolarization features comprise 40% of the top 25. Measures of entropy comprise 20% of the top 25, and 40% of the top repolarization features. The distribution of time, frequency and non-linear features is 24%, 24%, and 52%, respectively.

Discussion

We hypothesized that addition of ECG repolarization variability features, including TWA, to RR variability features would enhance the predictive capability for cardiac rearrest occurrence *and* rhythm type (No rearrest, PEA rearrest, or VT/VF rearrest) in a machine learning model. For the first time, we show that addition of repolarization features to RR variability features improved model performance in predicting rearrest occurrence. However, the addition of repolarization variability features generally did not improve model performance of the overall ML model in predicting rearrest type.

RR Variability to Predict Rearrest Occurrence – Comparison to Prior Studies:

Using the ECG to predict cardiac outcomes is very appealing because it is a cost effective, non-invasive measurement. Previous studies have shown that ECG depolarization such as late potentials in the QRS wave[11] and repolarization such as T-wave alternans[23-25,27,43-44], and QT dispersion[53] can be effective. However, none so far are fully accepted. With the development of ML, numerous studies have been able to detect major adverse cardiac events (e.g., arrhythmias) from the ECG, and some have shown that events can be predicted[40-41]. *Elola et al* is the first and only study to predict

rearrest occurrence using 17 RR variability features calculated from the ECGs of out-of-hospital CA patients. We confirmed that RR variability is a useful tool for predicting rearrest occurrence. They report an AUROC of 0.69, which we confirmed when using a similar ensemble classifier. RR variability features SD2 and entropy were both among the top 5 most important features for both our study and *Elola et al.*

The most important RR variability features in our study were RR interval range, followed by SD2 and standard deviation. We speculate that higher variability for RR interval range, SD2, and standard deviation is associated with rearrest. Considering our analysis window is ≤ 2 minutes, high variation over a short duration with minimal change in external activity likely indicates abnormally high RR variability and may be a marker for impending rearrest. The sample Poincaré plot (Figure 12) shows SD2 is increased for the patient who had PEA rearrest compared to the patient who did not rearrest. Other studies have reported increased RR variability is associated with increased risk of mortality and atrial fibrillation[54,55]. Additionally, *Elola et al* reported increased variability in features like SD2 and standard deviation of the RR interval series, further supporting the observation that increased RR variability is a marker for and likely linked to a mechanism of rearrest. This is in contrast to what most HRV studies report, which examine the relationship between HRV and longer

term risk of CA. Typically, these studies demonstrate that decreased HRV is linked to increased risk of CA. However, these studies analyze HRV on ECGs over a 24 hour period and are not applied to acute (within minutes) risk of sudden CA, but rather long term risk. Increased HRV is associated with increased parasympathetic tone whereas decreased HRV is associated with increased sympathetic tone, which is likely very high post CA, due to both intrinsic response to resuscitation and external factors such as administration of epinephrine and defibrillation. Enhancement of sympathetic tone will increase atrial and ventricular excitability and presence of ectopic beats will increase HRV, potentially exacerbated by impaired parasympathetic modulation. So although increased HRV may be associated with rearrest, this result may not be due to parasympathetic factors, but rather increased sympathetic modulation. Our recordings were very short, and included non-sinus beats, where typically only long recordings of sinus beats are used to determine HRV. Therefore, physiological interpretation of these results relative to other studies examining HRV and arrhythmia risk must be done with care.

Addition of Repolarization Variability Features to Predict Rearrest Occurrence & Type:

Abnormalities of ECG T-wave are well known to be associated with poor cardiac outcomes[18,23-29,35,43,44]. Adding repolarization variability features to RR variability improved predictive capacity for rearrest occurrence. Model performance metrics improved, including specificity (No RA) (53% to 59%) and validation accuracy (64% to 66%). Additionally, repolarization variability features were well represented in the top 25 overall, suggesting they have important qualities that distinguish rearrest from no rearrest. These results support our hypothesis that adding repolarization variability features will improve predictive capability for cardiac rearrest *occurrence* when compared to RR variability features alone.

For predicting rearrest type, addition of repolarization variability features to RR variability features generally did not improve predictive capacity. In this case, only one performance metric improved: specificity for the VT/VF rearrest group (92% to 96%). All other performance metrics decreased, although some nevertheless remained high (sensitivity of No RA, specificity of PEA RA). These results do not support our hypothesis that addition of repolarization variability features will improve predictive

capability for rearrest *type* (no rearrest, PEA rearrest, VT/VF rearrest) over RR variability features alone. Despite this, repolarization features were well represented in the top 25 overall at 44%. Compared to the number of features among the top 25 used to predict rearrest *occurrence*, the number used to predict rearrest *type* increased (9 to 11). These results suggest that repolarization variability features remain important in differentiating rearrest type, however the PEA and VT/VF rearrest classes may not be linearly separable. This could also explain the low performance of the baseline classifier that used RR variability features to predict rearrest type.

Alternatively, these results could imply that the calculated features (both RR variability and repolarization variability) do not sufficiently distinguish the PEA and VT/VF rearrest classes. One explanation for why the calculated features may not distinguish PEA from VT/VF is changing dynamics of the ECG. As an example, if TWA is only present for 15 seconds of a 2 minute window, the average oscillation amplitude will tend towards zero because the majority of the trace had no TWA. Assuming the hypothesized differences between rearrest classes exist, the nature of feature calculation over a long analysis windows could mask these results. Future work includes segmenting analysis windows based on changes in ECG stationarity to effectively isolate significant events, like transient TWA, which may help separate the

classes. Some studies have used segmented analysis on the ECG or cardiac action potential recordings, using fixed windows of short duration[40,41]. No studies are currently known to use ECG segments based on changes in signal dynamics for prediction of rearrest occurrence or type using ML. This provides a unique opportunity to identify the presence, occurrence, and duration of transient repolarization patterns that we have shown to be strongly associated with rearrest occurrence and type.

Non-Linear Repolarization Features & Entropy:

The top 25 ANOVA ranked features provided valuable insight into feature types and characteristics that were important to predicting rearrest occurrence and type. Of the repolarization variability features included in the top 25 overall, non-linear was the most dominant feature type. In predicting rearrest occurrence, 64% of the top repolarization features were non-linear. Similarly, for predicting rearrest type, 89% of the top repolarization features were non-linear. These results may implicate important non-linear physiologic processes, such as calcium transient alternans, which underpin the development of arrhythmias that lead to cardiac rearrest. Other studies have implicated the importance of non-linear dynamics in arrhythmia

development[56,57]. Further investigation is needed to fully comprehend and consider these results in the context of this study.

Of the non-linear features, sample entropy of the QT interval, T-wave amplitude, repolarization area, and 4:1 T-wave oscillation amplitude series were the most prevalent of the top repolarization features for predicting rearrest occurrence and type, with sample entropy of the QT interval series being the single most important ANOVA ranked feature in both models. Sample entropy estimates the degree of randomness, or lack thereof via predictable patterns, in each repolarization series. This suggests that the repolarization patterns of some groups are more predictable than others. We had proposed that alternations or oscillations in T-wave amplitude would precede cardiac rearrest occurrence. More specifically, alternating patterns of T-wave amplitude (TWA) may be a marker for mechanical dysfunction and PEA rearrest, while complex patterns of T-wave amplitude may be a biomarker for VT/VF rearrest (see *Repolarization Patterns to Predict Cardiac Outcomes*). Although the methods in this study were unable to identify whether specific patterns (TWA or complex) were associated with specific rearrest types (PEA or VT/VF), the importance of features like sample entropy support the idea that predictable patterns of repolarization exist and that unique patterns distinguish the groups. Further analysis

can be directed at elucidating the types of repolarization patterns that are associated with rearrest occurrence and type and will be considered for future work.

Clinical Implications from Machine Learning:

Although the classifier predicting rearrest type had generally poor performance, important clinical implications can still be considered with these results. The median performance of the classifier used to predict rearrest type showed high sensitivity for the no rearrest group (94%), and high specificity for the PEA and VT/VF rearrest groups (90%, 96%). This implies the classifier is good at correctly classifying observations that did not rearrest and good at correctly excluding observations that did not have a PEA or VT/VF rearrest. This suggests that the model will have a high probability of correctly classifying observations that truly belong to the PEA and VT/VF rearrest groups.

These results could have important clinical implications with regard to prophylactic treatments to prevent rearrest depending on the underlying mechanism. With high sensitivity for correctly detecting patients who will not rearrest, clinicians could withhold further treatments which would have no benefit and only expose patients to adverse effects of some unnecessary therapies. For example,

antiarrhythmic drugs can decrease ventricular contractile function, potentially predisposing a patient to PEA, while epinephrine by further increasing sympathetic tone, can promote VT/VF[9,10]. However, with a low false positive rate for the PEA and VT/VF rearrest groups, when a patient is identified as belonging to one of those groups, the benefit of prophylactic antiarrhythmics or vasopressors theoretically could outweigh the potential risk and abate the impending rearrest, which clearly worsens outcomes. Unfortunately, as currently developed, once the model identifies rearrest, it cannot decipher PEA from VT/VF. Clinically, this makes it difficult to apply targeted treatments based on rearrest type. Moreover, in the future, clinical features may be used to improve the ML algorithm. For example, primary arrest rhythm was identified in our study as a highly sensitive marker for VT/VF rearrest and it is likely that incorporating this, or other potential resuscitation/clinical parameters could significantly improve the model's correct identification of rearrest type. Additionally, these models could potentially be used to predict impending arrhythmias or primary CA in patients who present with other conditions such as acute heart failure or ischemic chest pain and have not yet had an arrhythmia or CA. Ultimately, machine learning algorithms such as those explored in this study could be implemented into

clinical monitoring equipment to identify patients who are at risk for rearrest occurrence and possibly rearrest type in real time.

Conclusions:

Our study confirmed, by showing equivalent performance to *Elola et al* [19] that RR variability features can be used in a ML model to successfully predict rearrest occurrence. Compared to RR variability alone, addition of repolarization variability features with feature selection improved prediction of rearrest occurrence as evidenced by improved model specificity and validation accuracy (Figures 20, 21), supporting our primary hypothesis. Prediction of rearrest type using RR variability features alone in a ML model was generally poor as given by low rearrest sensitivity and validation accuracy (Table 8). The addition repolarization variability features with feature selection did not improve prediction of rearrest type as evidenced by decreased validation accuracy, AUROC, and rearrest sensitivity, in contrast to our secondary hypothesis (Figure 23). Nevertheless, identification of the top 25 most important ANOVA ranked features demonstrated that repolarization features were strongly associated with both rearrest occurrence and type (Figures 22, 24). With further development and refined clinical implementation, machine learning models

represent a potential novel method of predicting rearrest and improving resuscitation outcomes.

Future Directions:

In order to improve the ML model, we plan to determine the causes underlying the lack of separability between the PEA and VT/VF rearrest classes. Additionally, predictability of rearrest and rearrest class may be improved by examining changing dynamics of the features by exploring the utility of segmenting the ECG to better capture transient, amplifying, or diminishing phenomena that may be related to rearrest occurrence and type. Finally, we plan to determine the statistical differences of response classes for the top features identified by the ANOVA ranking algorithm and potentially explore the use of additional descriptors, such as phase space analysis, which captures important underlying nonlinear dynamics that may implicate arrhythmia development. Finally, testing and modifying this model to predict primary cardiac arrest, a significant clinical problem, would be an very important next step.

Bibliography

1. Zipes, D. P., & Wellends, H. J. (1998). Sudden Cardiac Death. *Circulation*, 2334-2350.

2. *What is Cardiac Arrest*. (2022, May 19). Retrieved from National Heart, Lung and Blood Institute: https://www.nhlbi.nih.gov/health/cardiac-arrest

3. Association, A. H. (2020). *Advanced Cardiac Life Support Provider Manual.*

4. Association, A. H. (2005). Management of Cardiac Arrest. *Circulation*, IV-58-IV-66.

5. Aehlert, B. (2018). *ECGs Made Easy 6th Edition.* Elsevier.

6. Myerburg, R. J., Halperin, H., Egan, D. A., Boineau, R., Chugh, S. S., Gillis, A. M., . . . Zipes, D. P. (2013). Pulseless Electrical Activity: Definition, Causes, Mechanisms, Management and Research Priorities for the Next Decade - Report From a National Heart, Lung, and Blood Institute Workshop. *Circulation*, 2532-2541.

7. Salcido, D. D., Sundermann, M. L., Koller, A. C., & Menegazzi, J. J. (2014). Incidence and outcomes of rearrest following out-of-hospital cardiac arrest. *Resuscitation*, 19-24.

8. van Alem, A. P., Post, J., & Koster, R. W. (2003). VF recurrence: characteristics and patient outcome in out-of-hospital cardiac arrest. *Resuscitation*, 181-188.

9. Libby, P., Bonow, R. O., Mann, D. L., Ziipes, D. P., & Braunwald, E. (2008). *Braunwald's Heaert Disease: A Textbook of Cardiovascular Medicine Volume 1.* Philadelphia: Elsevier.

10. Tisdale, J. E., Patel, R. V., Webb, C. R., Borzak, S., & Zarowitz, B. J. (1995). Proarrhythmic Effects of Intravenous Vasopressors. *Annals of Pharmacotherapy*, 235-322.

11. Santangeli, P., Infusino, F., Sgueglia, G. A., Sestito, A., & Lanza, G. A. (2008). Ventricular Late Potentials: A Critical Overview and Current Applications. *Journal of Electrocardiography*, 318-324.

12. Huikuri, H. V., Makikallio, T., Airaksinen, K., Mitrani, R., Castellanos, A., & Myerburg, R. J. (1999). Measurement of Heart Rate Variability: A Clinical Tool or a Research Toy? *Journal of the American College of Cardiology*, 1878-1883.

13. Task Force of the European Society of Cardiology, t. N. (1996). Heart Rate Variability Standards of Measurement, Physiological Interpretation, and Clinical Use. *Circulation*, 1043-1065.

14. Shaffer, F., & Ginsberg, J. P. (2017). An Overview of Heart Rate Variability Metrics and Norms. *Frontiers in Public Health*.

15. Shusterman, V., Aysin, B., Gottipaty, V., Weiss, R., Brode, S., Schwartzman, D., & Anderson, K. P. (1998). Autonomic Nervous System Activity and the Spontaneous Initiation of Ventricular Tachycardia. *Journal of the American College of Cardiology*, 1891-1899.

16. Huikuri, H. V., Seppanen, T. M., Koistinen, J., Airaksinen, K., Ikäheimo, M., Castellanos, A., & Myerburg, R. J. (1996). Abnormalities in Beat-to-Beat Dynamics of Heart Rate Before the Spontaneous Onset of Life-Threatening Ventricular Tachyarrhythmias in Patients With Prior Myocardial Infarction. *Circulation*, 1836–1844.

17. Valkama, J. O., Huikuri, H. V., Koistinen, J., Yli-Mayry, S., Airaksinen, K., & Myerburg, R. J. (1995). Relation Between Heart Rate Variability and

Spontaneous and Induced Ventricular Arrhythmias in Patients With Coronary Artery Disease. *Journal of the American College of Cardiology*, 437-443.

18. Do, D. H., Kuo, A., Lee, E. S., Mortara, D., Elashoff, D., Hu, X., & Boyle, N. G. (2019). Usefulness of Trends in Continuous Electrocardiographic Telemetry Monitoring to Predict In-Hospital Cardiac Arrest. *The American Journal of Cardiology*, 1149-1158.

19. Elola, A., Aramendi, E., Rueda, E., Irusta, U., Wang, H., & Idris, A. (2020). Towards the Prediction of Rearrest During Out-of-Hospital Cardiac Arrest. *Entropy*.

20. Landstedt-Hallin, L., Englund, A., Adamson, U., & Lins, P. E. (1999). Increased QT dispersion during hypoglycaemia in patients with type 2 diabetes mellitus. *Journal of Internal Medicine*, 299-307.

21. Alerhand, S., Adrian, R. J., Long, B., & Avila, J. (2022). Pericardial tamponade: A comprehensive emergency medicine and electrocardiography review. *American Journal of Emergency Medicine*, 159-174.

22. Coustet, B., Lhuissier, F. J., Vincent, R., & Richalet, J.-P. (2015). Electrocardiographic Changes During Exercise in Acute Hypoxia and Susceptibility to Severe High-Altitude Illnesses. *Circulation*, 786-794.

23. Rosenbaum, D. S., Jackson, L. E., Smith, J. M., Garan, H., Ruskin, J. N., & Cohen, R. J. (1994). Electrical Alternans and Vulerability to Ventricular Arrhythmias. *The New England Journal of Medicine*, 235-241.

24. Narayan, S. M. (2006). T-Wave Alternans and the Susceptibility to Ventricular Arrhythmias. *Journal of the American College of Cardiology*, 269-281.

25. Nearing, B. D., & Verrier, R. L. (2002). Progressive Increases in Complexity of T-wave Oscillations Herald Ischemia-Induced Ventricular Fibrillation. *Circulation Research*, 727-732.

26. Bayer, J., Lalani, G., Vigmond, E., Narayan, S., & Trayanova, N. (2016). Mechanisms linking electrical alternans and clinical ventricular arrhythmia in human heart failure. *Heart Rhythm Society*, 1922-1931.

27. Nearing, B. D., & Verrier, R. L. (2002). Modified moving average analysis of T-wave alternans to predict ventricular fibrillation with high accuracy. *Journal of Applied Physiology*, 541-549.

28. Wilson, L. D., & Rosenbaum, D. S. (2007). Mechanisms of Arrhythmogenic Cardiac Alternans. *European Society of Cardiology*, vi77-vi82.

29. Cutler, M. J., & Rosenbaum, D. S. (2008). Explaining the clinical manifestations of T wave alternans in patients at risk for sudden cardiac death. *2008*, S22-S28.

30. Weiss, J. N., Karma, A., Shiferaw, Y., Chen, P.-S., Garfinkel, A., & Qu, Z. (2006). From Pulsus to Pulseless The Saga of Cardiac Alternans. *Circulation Research*, 1244-1253.

31. Gaeta, S. A., Bub, G., Abbott, G. W., & Christini, D. J. (2009). Dynamical Mechanisms for Subcellular Alternans in Cardiac Myocytes. *Circulation Research*, 335-342.

32. Weiss, J. N., Nivala, M., Garfinkel, A., & Qu, Z. (2011). Alternans and Arrhythmias From Cell to Heart. *Circulation Research*, 98-112.

33. Wilson, L. D., Wan, X., & Rosenbaum, D. S. (2006). Cellular Alternans A Mechanismm Linking Calcium Cycling Proteins to Cardiac Arrhythmogenesis. *Annals New York Academy of Sciences*, 216-234.

34. Cutler, M. J., Wan, X., Laurita, K. R., Hajjar, R. J., & Rosenbaum, D. S. (2009). Targeted SERCA2a Gene Expression Identifies Molecular Mechanism and Therapeutic Target for Arrhythmogenic Cardiac Alternans. *Circulation: Arrhythmia and Electrophysiology*, 686-694.

35. Pastore, J. M., Girouard, S. D., Laurita, K. R., Akar, F. G., & Rosenbaum, D. S. (1999). Mechanism Linking T-wave Alternans to the Genesis of Cardiac Fibrillation. *Circulation*, 1385-1394.

36. Zhou, X., Bueno-Orovio, A., Orini, M., Hanson, B., Hayward, M., Taggart, P., . . . Rodriguez, B. (2015). In Vivo and In Silico Investigation Into Mechanisms of Frequency Dependence of Repolarization Alternans in Human Ventricular Cardiomyocytes. *Circulation Research*, 266-278.

37. Chudin, E., Goldhaber, J., Garfinkel, A., Weiss, J., & Kogan, B. (1999). Intracellular Calcium Dynamics and the Stability of Ventricular Tachycardia. *Biophysical Journal*, 2930-2941.

38. Oshodi, G. O., Wilson, L. D., Costantini, O., & Rosenbaum, D. S. (2008). Microvolt T Wave Alternans: Mechanisms and Implications for Prediction of Sudden Cardiac Death. In I. Gussak, C. Antzelevitch, A. Wilde, P. Friedman, M. Ackerman,

& W.-K. Shen, *Electrical Diseases of the Heart: Genetics, Mechanisms, Treatment, Prevention.* Springer.

39. Patil, K., Halperin, H. R., & Becker, L. B. (2015). Cardiac Arrest: Resuscitation and Reperfusion. *Circulation Research*, 2041-2049.

40. Rogers, A. J., Selvalingham, A., Alhusseini, M. I., Krummen, D. E., Corrado, C., Abuzaid, F., . . . Narayan, S. M. (2021). Machine Learned Cellular Phenotypes in Cardiomyopathy Predict Sudden Death. *Circulation Research*, 172-184.

41. Urteaga, J., Aramendi, E., Elola, A., Irusta, U., & Idris, A. (2021). A Machine Learning Model for the Prognosis of Pulseless Electrical Activity during Out-of-Hospital Cardiac Arrest. *Entropy*.

42. Delgado-Bonal, A., & Marshak, A. (2019). Approximate Entropy and Sample Entropy: A Comprehensive Tutorial. *Entropy*.

43. Nearing, B. D., Huang, A. H., & Verrier, R. L. (1991). Dynamic Tracking of Cardiac Vulnerability by Complex Demodulation of the T wave. *Science*, 437-440.

44. Nearing, B. D., & Verrier, R. L. (1993). Personal computer system for tracking cardiac vulnerability by complex demodulation of the T wave. *Journal of Applied Physiology*, 2606-2612.

45. James, G., Witten, D., Hastie, T., & Tibshirani, R. (2017). *An Introduction to Statistical Learning with Applications in R.* Springer.

46. Wolbinski, M., Swain, A. H., Harding, S. A., & Larsen, P. D. (2016). Out-of-hospital Cardiac Arrest Patient Characteristics: Comparing ventricular arrhythmia and Pulseless Electrical Activity. *Heart, Lung and Circulation*, 639-644.

47. Daya, M. R., Schmicker, R. H., Zive, D. M., Rea, T. D., Nichol, G., Buick, J. E., . . . Wnag, H. (2015). Out-of-hospital cardiac arrest survival improving over time: Results from the Resuscitation Outcomes Consortium. *Resuscitation*, 108-115.

48. Keller, S. P., & Halperin, H. R. (2015). Cardiac Arrest: the Changing Incidence of Ventricular. *Current Treatment Options in Cardiovascular Medicine*.

49. Kauppila, J. P., Hantula, A., Kortelainen, M.-L., Pakanen, L., Perkiomaki, J., Martikainen, M., . . . Junttila, M. (2018). Association of initial recorded rhythm and underlying cardiac disease in sudden cardiac arrest. *Resuscitation*, 76-78.

50. Empana, J.-P., Lerner, I., Valentin, E., Folke, F., Bottiger, B., Gislason, G., . . . Jouven, X. (2022). Incidence of Sudden Cardiac Death in the European Union. *Journal of the American College of Cardiology*, 1818-1827.

51. Stoecklein, H. H., Pugh, A., Johnson, M. A., Tonna, J. E., Stroud, M., Drakos, S., & Youngquist, S. T. (2022). Paramedic rhythm interpretation misclassification is associated with poor survival from out-of-hospital cardiac arrest. *Resuscitation*, 33-40.

52. Salcido, D. D., Stephenson, A. M., Condle, J. P., Callaway, C. W., & Menegazzi, J. J. (2010). Incidence of Re-arrest after Return of Spontaneous Circulation in Out-of-Hospital Cardiac Arrest. *Prehospital Emergency Care*, 413-418.

53. Shah, B. R., Yamazaki, T., Engel, G., Cho, S., Chun, S. H., & Froelicher, V. F. (2004). Computerized QT Dispersion Measurement and Cardiovascular Mortality in Male Veterans. *American Journal of Cardiology*, 483-486.

54. Stein, P. K., Domitrovich, P. P., Hue, N., Rautaharju, P., & Gottdiener, J. (2005). Sometimes Higher Heart Rate Variability is Not Better Heart Rate Variability: Results of Graphical and Non-Linear Analysis. *Journal of Cardiovascular Electrophysiology*, 954-959.

55. Kim, S. H., Lim, K. R., Seo, J.-H., Ryu, D. R., Lee, B.-K., Cho, B.-R., & Chun, K. J. (2022). Higher heart rate variability as a predictor of atrial fibrillation in patients with hypertension. *Scientific Reports*.

56. Krogh-Madsen, T., & Christini, D. J. (2012). Nonlinear Dynamics in Cardiology. *Annual Reviews Biomedical Engineering*, 179-203.

57. Ravelli, F., & Antolini, R. (1992). Complex dynamics underlying the human electrocardiogram. *Biological Cybernetics*, 57-65.